

Cyclohydroamination of Aminoalkenes Catalyzed by Disilazide Alkaline-Earth Metal Complexes: Reactivity Patterns and Deactivation Pathways

Bo Liu,^[a] Thierry Roisnel,^[b] Jean-François Carpentier,^{*,[a]} and Yann Sarazin^{*,[a]}

Abstract: The behavior of the first aminophenolate catalysts of the large alkaline earth metals (Ae) [(LO^δ)AeN(SiMe₂R)₂(thf)_x] (*i* = 1–4; Ae = Ca, Sr, Ba; R = H, Me; *x* = 0–2) for the cyclohydroamination of terminal aminoalkenes is discussed. The complexes [(BDI)AeN(SiMe₂H)₂(thf)_x] (Ae = Ca, Sr, Ba, *x* = 1–2; (BDI)H = H₂C[C(Me)N-2,6-(*i*Pr)₂C₆H₃]₂) and [(BDI)CaN(SiMe₃)₂(thf)] supported by the β-diketiminato (BDI)[−] ligand have also been employed for comparative and mechanistic considerations. The catalytic performances decrease in the order Ca > Sr >> Ba, which is the opposite trend to that previously observed during the intermolecular hydroamination of activated alkenes catalyzed by the same alkaline-earth metal complexes. Catalyst efficacy increases when the chelating and donating ability of the aminophenolate ligands decreases. For given metals and ancillary scaffolds, disilazide catalysts that incorporate the N(SiMe₃)₂[−] amido group out-

class their congeners containing the N(SiMe₂H)₂[−] amide owing to the lower basicity of the N(SiMe₂H)₂[−] with respect to the N(SiMe₃)₂[−] group, and also because Ae–N(SiMe₂H)₂ catalysts suffer from irreversible deactivation through the dehydrogenative coupling of amine and hydrosilane moieties. This deactivation process takes place at 25 °C in the case of [(LO^δ)AeN(SiMe₂H)₂(thf)_x] phenolate complexes and occurs even with the related [(BDI)AeN(SiMe₂H)₂(thf)_x] complex, albeit under conditions harsher than those required for effective cyclohydroamination catalysis. A mechanistic scenario for cyclohydroamination catalyzed by [(LX)AeN(SiMe₂H)₂(thf)_x] complexes ((LX)[−] = (LO^δ)[−] or (BDI)[−]) is proposed. Although beneficial for

the synthesis of Ae heteroleptic complexes able to resist deleterious Schlenk-type equilibria, the use of the N(SiMe₂H)₂[−] is prejudicial to catalytic activity in the case of catalyzed transformations that involve reactive amine (and potentially other) substrates. Mechanistic and kinetic investigations further illustrate the interplay between the catalytic activity, operative mechanism, and identity of the metal, ancillary ligand, and amido group. These studies suggest that the widely accepted mechanism for cyclohydroamination reactions cannot be extended systematically to all alkaline-earth catalysts. The [(BDI)CaN(SiMe₂H)₂{H₂NCH₂C(CH₃)₂CH=CH₂}] complex, the first Ca–aminoalkene adduct structurally characterized, was prepared quantitatively and essentially behaves like [(BDI)CaN(SiMe₂H)(thf)], thus serving as a model compound for mechanistic studies, as illustrated during stoichiometric reactions monitored by ¹H NMR spectroscopy.

Keywords: alkaline-earth metals • alkenes • amido complexes • cyclohydroamination • reaction mechanisms

Introduction

Atom-efficient catalyzed hydroamination reactions, which afford the formation of valuable nitrogen-containing com-

pounds^[1] by addition of an N–H bond across unsaturated carbon–carbon linkages, have become something of a hot topic.^[2] Following the seminal work of Marks and co-workers with rare-earth metal complexes,^[2b,3] catalysts based on metals spanning across almost the entire Periodic Table have been reported to mediate these very slightly exothermic but otherwise entropically unfavorable reactions.^[2] Late-transition metals have shown characteristic robustness and functional group tolerance and can promote the regioselective, and sometimes stereoselective, Markovnikov addition of amines to nonactivated alkenes.^[2c,d] On the other hand, catalysts based on oxophilic metals typically display high reaction rates.^[2a-c,3-5] Perhaps more strikingly, rare-earth metal complexes generate linear products through regioselective anti-Markovnikov addition of amines to activated olefins. Nearly two decades have elapsed since this reaction was identified as one of the “Ten Challenges in Catalysis” by Haggin,^[6] and yet the breakthroughs required to

[a] Dr. B. Liu, Prof. Dr. J.-F. Carpentier, Dr. Y. Sarazin
Organometallics: Materials and Catalysis
Institut des Sciences Chimiques de Rennes
UMR 6226 CNRS, Université de Rennes 1
Campus de Beaulieu, Rennes, 35042 Cedex (France)
Fax: (+33) (0)2 23 23 69 39
E-mail: jean-francois.carpentier@univ-rennes1.fr
yann.sarazin@univ-rennes1.fr

[b] Dr. T. Roisnel
Centre de Diffractométrie X
Institut des Sciences Chimiques de Rennes
UMR 6226 CNRS, Université de Rennes 1
Campus de Beaulieu, Rennes, 35042 Cedex (France)

Supporting information for this article is available on the WWW under <http://dx.doi.org/10.1002/chem.201203562>.

broaden the substrate scope, minimize catalyst loading, and optimize reaction rates have remained elusive.

In 2005, Hill, Barrett, and co-workers revealed that the ubiquitous β -diketiminato amido/calcium complex $[(\text{BDI})\text{CaN}(\text{SiMe}_3)_2(\text{thf})]^{[7]}$ ($(\text{BDI})\text{H} = \text{H}_2\text{C}\{\text{C}(\text{Me})\text{N}-2,6-(i\text{Pr})_2\text{C}_6\text{H}_3\}_2$) constitutes a very competent catalyst for the cyclohydroamination of aminoalkenes.^[8] In a series of remarkable contributions, they further elaborated on their initial success to demonstrate that the large alkaline-earth metals (Ae = Ca, Sr, and Ba) are particularly suited to the catalysis of a range of hydroelementation reactions,^[9,10] and they provided useful insight into the mechanisms that operate with complexes of these metals.^[9g] In a similar manner to their next-of-kin the rare-earth and alkali metals, the coordination chemistry of the large (ionic radii for coordination number (CN) = 6: 1.00, 1.18, and 1.35 Å for Ca^{2+} , Sr^{2+} , and Ba^{2+} , respectively),^[11] electropositive, and highly polarizable Ca–Ba elements is largely governed by electrostatic and steric factors; consequently, bonding is essentially non-directional and highly ionic. The authors showed that Ca catalysts frequently, but not systematically, exhibited better catalytic performances than their (Mg) Sr and Ba analogues for hydroamination reactions. However, one notable exception was the intermolecular hydroamination of activated alkenes, in which Sr catalysts outclassed Ca catalysts.^[9e,g-h] No clear pattern for reactivity versus metal size could therefore be established, even if it appeared that the Mg and Ba catalysts were always rather mediocre. In analogy with the rare-earth systems developed by Marks and co-workers, the alkaline-earth catalysts developed by Hill and co-workers followed the rules developed by Baldwin for ring-closure during cyclohydroamination reactions and also promoted the anti-Markovnikov intermolecular hydroamination of vinylarenes and dienes.^[9]

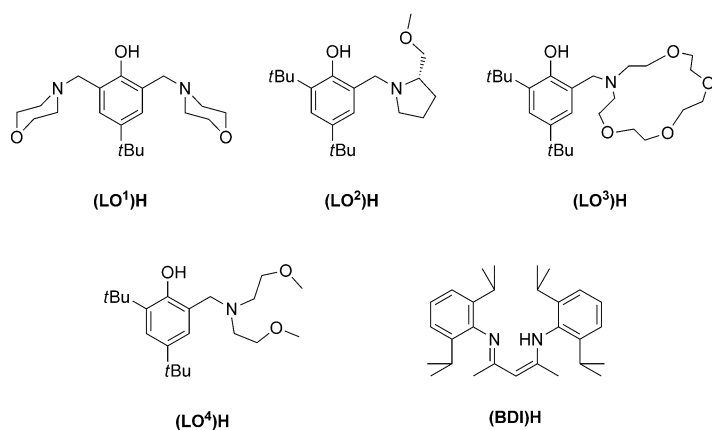
In the wake of the promising accounts of Hill and Barrett, several research groups have become involved in the development of large Ae (Ca, Sr, Ba)^[12] catalysts supported by nitrogen-containing ancillaries for hydroamination reactions. Roesky and co-workers reported that Ca catalysts outperformed their Sr analogues in cyclohydroamination reactions catalyzed by heteroleptic aminotroponimate^[13] or 2,5-bis-[N-(aryl)iminomethyl]pyrrolyl^[14] complexes. Moderate enantioselectivity (i.e., 12–26% *ee*) was observed by Wixey and Ward in the cyclohydroamination of aminoalkenes with Ca catalysts bearing chiral 1,2-diamine^[15] or bisimidazoline^[16] ligands,^[17] but their kinetic stability was somewhat limited, an issue often encountered in Ae coordination chemistry, in which deleterious Schlenk-type equilibria are troublesome.^[18] To our knowledge, Ca–Ba phenolate complexes have never been employed for cyclohydroamination reactions, although Hultsch and co-workers recently achieved highly enantioselective reactions with a chiral Mg parent.^[12d] Beyond catalytic hydroamination, Ca–Ba catalysts have also displayed notable efficacy in hydrosilylation,^[19] alkene hydrogenation,^[20] or styrene^[21] and cyclic esters^[7,18a,22] polymerization reactions in the past decade or so, which is a testimony to the growing importance of this field.

As part of a program to implement new catalyst systems for atom-efficient reactions, we became interested in developing ways to stabilize electron-deficient alkaline-earth species. We found that Ae \cdots H–Si β -agostic interactions in charge-neutral heteroleptic alkaline-earth metal complexes of the type $[(\text{LX})\text{AeN}(\text{SiMe}_2\text{H})_2]$ (Ae = Ca, Sr, Ba; (LX)[−] = monoanionic ancillary aminophenolate, iminoanilide, or β -diketiminato ligand) constitute an effective way to prevent solution ligand redistribution reactions that are too frequently observed with their $[(\text{LX})\text{AeN}(\text{SiMe}_3)_2]$ congeners and that these complexes are potent catalysts for ring-opening polymerization,^[22k,n] hydrophosphonylation,^[23] or intermolecular hydroamination and hydrophosphination reactions.^[24] We were surprised to observe that reaction rates increased linearly with the size of the metal center in these catalyzed reactions, whereas the selectivity was maintained.^[25] In contrast with the earlier predictions of Hill and co-workers based on DFT computations and observations made with $[\text{Ae}\{\text{N}(\text{SiMe}_3)_2\}_2(\text{thf})_x]$ (Ae = Ca, Sr, Ba; $x = 0, 2$),^[9e,h] we noticed that this trend was particularly pronounced in intermolecular hydroamination reactions. The Ba catalysts performed systematically better than Sr and, to a greater extent, Ca catalysts in three complete families of stable $[(\text{LX})\text{AeN}(\text{SiMe}_3)_2]$ complexes supported by various ligand scaffolds, thus yielding linear products after the regio-specific anti-Markovnikov addition of the amine group to the C=C unsaturation.^[24]

Herein, we report that Ca, Sr, and Ba heteroleptic $[(\text{LX})\text{AeN}(\text{SiMe}_2\text{R})_2(\text{thf})_x]$ (R = H, Me) complexes bearing aminophenolate ligands are active catalysts in the cyclohydroamination of aminoalkenes and show that reaction rates decrease regularly on moving from Ca to Ba in this intramolecular version of hydroamination reactions. The behavior of these catalysts is compared to that of their β -diketiminato analogues, the roles of the supporting ligand and of the NR_2^- moiety are questioned, and a mechanistic scenario that highlights a specific catalyst deactivation pathway is proposed.

Results and Discussion

Catalyst selection and syntheses: Four proligands (LO)^hH were selected for the preparation of alkaline-earth metal catalysts on account of their varying chelating abilities and stereoelectronic properties (Figure 1). Because it is the benchmark proligand in this area, (BDI)H was also used for comparative purposes. As they revealed high efficiency in the intermolecular hydroamination of activated alkenes,^[24] the complexes $[(\text{LO}^h)\text{AeN}(\text{SiMe}_3)_2(\text{thf})_x]$ (Ae = Ca, $x = 0$ (**1**); Sr, $x = 1$ (**2**); Ba, $x = 0$ (**3**)) containing the tetradentate phenolate (LO)^h were picked as our catalysts of choice for initial screening. To assess the importance of the identity of the amide group attached to the metal center, the complexes $[(\text{LO}^h)\text{CaN}(\text{SiMe}_2\text{H})_2(\text{thf})_x]$ (**4**) and the dimeric $[(\text{LO}^h)\text{AeN}(\text{SiMe}_2\text{H})_2]_2$ (Ae = Sr (**5**)₂; Ba (**6**)₂) were also selected. Although it shows some signs of decomposi-



$[(LO^4)CaN(SiMe_3)_2]$	1	$[(LO^1)CaN(SiMe_2H)_2]_2$ (7) ₂	$[(BDI)CaN(SiMe_2H)_2(thf)]$	11	
$[(LO^4)SrN(SiMe_3)_2(thf)]$	2	$[(LO^2)CaN(SiMe_2H)_2]_2$ (8)	$[(BDI)SrN(SiMe_2H)_2(thf)_2]$	12	
$[(LO^4)BaN(SiMe_3)_2]$	3	$[(LO^3)CaN(SiMe_2H)_2]$	9	$[(BDI)BaN(SiMe_2H)_2(thf)_2]$	13
$[(LO^4)CaN(SiMe_2H)_2(thf)]$	4	$[(LO^1)CaN(SiMe_3)_2]_2$ (10) ₂			
$[(LO^4)SrN(SiMe_2H)_2]_2$	(5) ₂		$[(BDI)CaN(SiMe_3)_2(thf)]$		
$[(LO^4)BaN(SiMe_2H)_2]_2$	(6) ₂				

Figure 1. Proligands and related complexes employed in this study for cyclohydroamination catalysis.

tion through Schlenk-type equilibria after periods of several days in solution, we found that the Ba complex **3** was sufficiently stable for catalytic reactions. In contrast, we have shown that the complete stability of its derivative **6** is warranted by a pattern of internal Ba⋯H-Si β-agostic interactions.^[22m] The Ca complex **4**, which contains an additional coordinated molecule of THF is stable, although Ca⋯H-Si agostic bonding was not established.^[22n] The new Sr complex (**5**)₂ was prepared in 73% yield by means of one-pot reaction of $[Sr\{N(SiMe_3)_2\}_2(thf)_2]$, (LO⁴)H, and HN(SiMe₂H)₂. It is very sparingly soluble in aromatic solvents. NMR spectroscopic data recorded in [D₈]THF show that the dimer splits partly in this coordinating solvent;^[26] furthermore, Van't Hoff analysis of the ¹H NMR spectroscopic data recorded in the temperature range 253–333 K gave values of 7.29 kJ mol⁻¹ and 5.5 J mol⁻¹ K⁻¹ for the dissociation enthalpy and entropy, respectively, with splitting of the dimer occurring spontaneously at elevated temperature.^[26]

The syntheses of the calcium complexes $[(LO^1)CaN(SiMe_2H)_2]_2$ (**(7)**)₂, $[(LO^2)CaN(SiMe_2H)_2]$ (**8**), $[(LO^3)CaN(SiMe_2H)_2]$ (**9**), and $[(LO^1)CaN(SiMe_2H)_2]_2$ (**(10)**)₂ have been described previously.^[22i,k,n] Pulse-gradient spin-echo NMR spectroscopic data indicated that these Ca species, dimeric in the solid state, split into monomeric species in aromatic solvents;^[22n] therefore, we made the assumption that this would be also the case under catalytic conditions. The complexes $[(LO^3)SrN(SiMe_2H)_2]$ and $[(LO^3)BaN(SiMe_2H)_2]$ were also already available,^[22k] but they eventually proved to be totally inert toward aminoalkenes. Besides, considering the activity versus ligand and activity versus metal trends observed during preliminary tests (see below), it did not

seem pertinent to proceed at this stage with the syntheses of Sr and Ba complexes bearing (LO¹)⁻ or (LO²)⁻ ligands. Instead, the complexes **1–3** and $[(BDI)AeN(SiMe_2H)_2(thf)_x]$ (Ae = Ca, x = 1 (**11**); Sr, x = 2 (**12**); Ba, x = 2 (**13**)) were compared. The latter species supported by the β-diketiminato ligand had previously proved to be substantially more active than phenolate or iminoanilide derivatives in the intermolecular version of hydroamination reactions.^[24] For comparative purposes, we also studied $[(BDI)CaN(SiMe_3)_2(thf)]$,^[7] the benchmark catalyst for intramolecular hydroamination with alkaline-earth-metal catalysis.^[9] The panel of catalysts employed in this study is displayed in Figure 1.

The $[(LO^4)SrN(SiMe_2H)_2]_2$ (**(5)**)₂ complex is a centrosymmetric dimer in the solid state (Figure 2), with a central {Sr₂O₂} planar core in which the two metal centers are bridged by the O_{phenoxide} atoms. There is some disorder in one of the {SiMe₂H} fragments (only the main component is depicted-

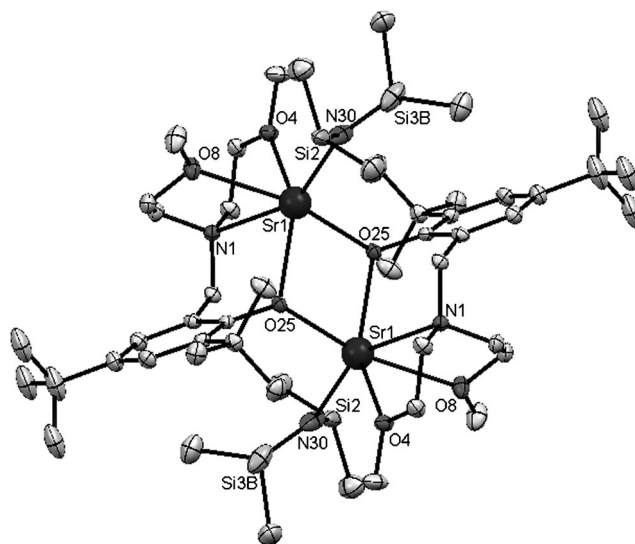


Figure 2. ORTEP diagram of the solid-state structure of $[(LO^4)SrN(SiMe_2H)_2]_2$ (**(5)**)₂. The noninteracting solvent molecule and hydrogen atoms are omitted for clarity. Ellipsoids are drawn at the 50% probability level; only the main components of disordered groups are depicted. Selected bond lengths [Å] and angles [°]: Sr1–O25#1 2.509(2), Sr1–O25 2.528(2), Sr1–N30 2.536(3), Sr1–O(4) 2.616(2), Sr1–O8 2.695(2), Sr1–N1 2.748(2), Sr1–Si3A 3.621(1), Sr1–N30 2.536(3); O25#1–Sr1–N30 105.01(8), O25–Sr1–O(4) 136.96(6), N30–Sr1–O8 93.60(8), O25#1–Sr1–N1 98.33(6), O8–Sr1–N1 62.98(6), Si2–N30–Sr1 117.2(2), Si3B–N30–Sr2 117.1(2).

ed in Figure 2). Each Sr atom is six-coordinate, as the ligand is bonded in a $\mu^2:\kappa^1,\kappa^4-N,O,O,O$ fashion to the metal center. The Sr–O_{phenoxide} distance of 2.53 Å is shorter than those to the O atoms of the side-arm ether groups (2.61–2.69 Å). The Sr1–N30 distance of 2.54 Å is far smaller than Sr1–N1 (2.75 Å). There is no clear evidence for the presence of Sr···H–Si agostic interactions in (**5**)₂,^[27] as the Sr1–N30–Si2 and Si3A–N30–Sr1 angles of 117.2(2)° and 117.1(2)° are equivalent. The two Sr–N–Si–H cores are coplanar, which could be seen as consistent with the presence of Sr···H–Si bonding involving both {SiMe₂H} moieties,^[27] but could also be the adventitious result of the minimization of steric factors.

The solid-state structure of the previously synthesized^[24] β-diketimate Sr complex **12** was also solved (Figure 3). Factors that corroborate the presence of Si···H–Si agostic bonding include a marked discrepancy between the two {SiMe₂H} groups (Si1–N1–Sr1: 104.8°, Si2–N1–Sr1: 127.4°; Sr1–Si1: 3.32 Å, Sr1–Si2: 3.74 Å) and the near coplanarity of the H–Si1–N1–Sr1 fragment (torsion angles: H–Si1–N1–Sr1 –9.8°; H–Si2–N1–Sr1 –31.9°).

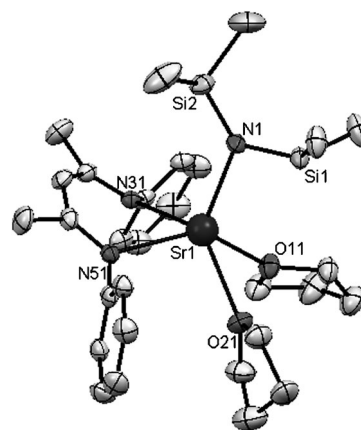
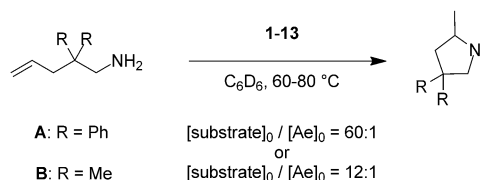


Figure 3. ORTEP diagram of the solid-state structure of [(BDI)SrN(SiMe₂H)₂(thf)₂] (**12**). The noninteracting solvent molecule, isopropyl groups on the BDI phenyl groups, and hydrogen atoms are omitted for clarity. Ellipsoids are drawn at the 50% probability level. Selected bond lengths [Å] and angles [°]: Sr1–N1 2.473(2), Sr1–N31 2.542(2), Sr1–N51 2.556(2), Sr1–O21 2.597(2), Sr1–O11 2.613(2), Sr1–H1 2.82(3); N1–Sr1–N31 104.32(6), N1–Sr1–N51 109.08(6), N1–Sr1–O21 119.80(7), N1–Sr1–O11 111.07(6), Si1–N1–Sr1 104.80(9), Si2–N1–Sr1 127.5(1).

Catalytic activity during cyclohydroamination: In a preliminary set of qualitative experiments, the catalytic ability of **1–13** in the cyclohydroamination of 1-amino-2,2-diphenyl-4-pentene (**A**) and 1-amino-2,2-dimethyl-4-pentene (**B**), two well-known substrates for which comparison with existing catalysts is possible, was investigated (Scheme 1). The reactions were carried out at 60 or 80 °C in [D₆]benzene with 1.7 or 8.3 mol% catalyst loading, and the conversion was monitored by ¹H NMR spectroscopy (Table 1).^[28] The initial assumption was that catalysts **1–13** would operate according to the commonly accepted mechanism depicted in Scheme 2.^[29]

The conversion of substrate **B** catalyzed by **1–3** is slower than that of **A**, as expected on account of the Thorpe–Ingold effect that favors cyclization for bulkier geminal substituents. In both cases, ring-closure proceeds according to the guidelines developed by Baldwin (5-*exo-trig*).

The cyclohydroamination of **A** catalyzed by Ca complex **1** at 80 °C was complete within less than 30 min (Table 1, entry 1), thus leading selectively to the formation of 2-methyl-4,4-diphenylpyrrolidine. By comparison, full conversion required one hour with the Sr analogue **2** (Table 1, entry 2), whereas only 10% conversion was achieved with Ba complex **3** (Table 1, entry 3) in that time. The activity trend was therefore

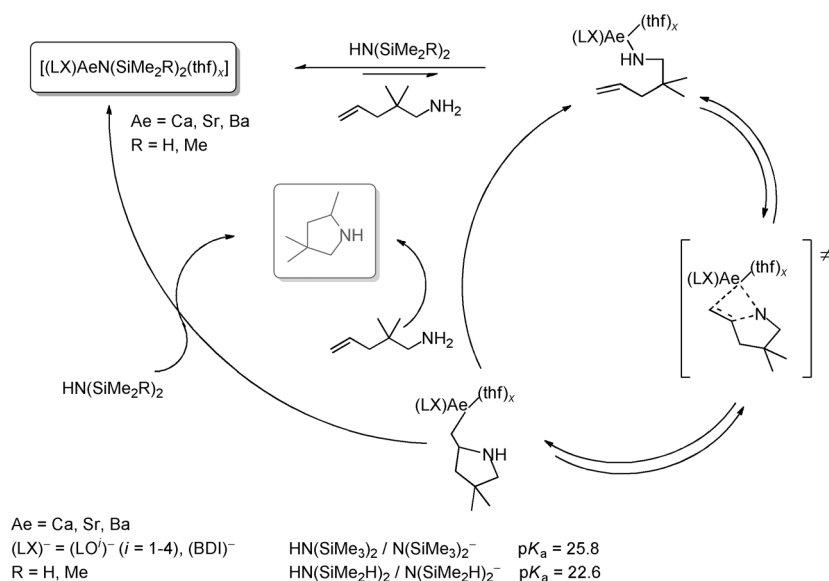


Scheme 1. Cyclohydroamination of 1-amino-2,2-diphenyl-4-pentene (**A**) and 1-amino-2,2-dimethyl-4-pentene (**B**) with catalysts **1–13**.

Table 1. Cyclohydroamination reactions catalyzed by **1–13**.

Entry	Catalyst	Substrate	[Substrate] ₀ / [Ae] ₀	T ^{re} [°C]	t [h]	Conv. ^[a] [%]
1 ^[b]	[(LO ⁴)CaN(SiMe ₃) ₂]	1	60	80	0.5	100
2 ^[b]	[(LO ⁴)SrN(SiMe ₃) ₂ (thf)]	2	60	80	1	99
3 ^[b]	[(LO ⁴)BaN(SiMe ₃) ₂]	3	60	80	1	10
4 ^[b]	[(LO ⁴)BaN(SiMe ₂ H) ₂] ₂	(6) ₂	60	80	1	6
5 ^[c]	[(BDI)CaN(SiMe ₃) ₂ (thf)]		60	60	5 min	>99
6 ^[b]	[(LO ⁴)CaN(SiMe ₃) ₂]	1	60	80	1.5	96
7 ^[b]	[(LO ⁴)SrN(SiMe ₃) ₂ (thf)]	2	60	80	5	99
8 ^[b]	[(LO ⁴)BaN(SiMe ₃) ₂]	3	60	80	5	31
9 ^[b]	[(LO ⁴)CaN(SiMe ₂ H) ₂ (thf)]	4	60	80	1.5	3
10 ^[b]	[(LO ⁴)CaN(SiMe ₂ H) ₂ (thf)]	4	60	80	25	70
11 ^[b]	[(LO ⁴)SrN(SiMe ₂ H) ₂] ₂	(5) ₂	60	80	5	61
12 ^[b]	[(LO ⁴)BaN(SiMe ₂ H) ₂] ₂	(6) ₂	60	80	5	18
13 ^[c]	[(LO ⁴)CaN(SiMe ₃) ₂] ₂	(10) ₂	12	60	3 min	99
14 ^[c]	[(LO ⁴)CaN(SiMe ₂ H) ₂] ₂	(7) ₂	12	80	12 min	99
15 ^[c]	[(LO ³)CaN(SiMe ₂ H) ₂]	8	12	80	1.5	98
16 ^[c]	[(LO ³)CaN(SiMe ₂ H) ₂]	9	12	80	36	0
17 ^[c]	[(LO ⁴)CaN(SiMe ₂ H) ₂ (thf)]	4	12	80	29	92
18 ^[c]	[(BDI)CaN(SiMe ₂ H) ₂ (thf)]	11	12	80	45 min	93
19 ^[c]	[(BDI)SrN(SiMe ₂ H) ₂ (thf) ₂]	12	12	80	3	91
20 ^[c]	[(BDI)BaN(SiMe ₂ H) ₂ (thf) ₂]	13	12	80	8	89

[a] Conversion determined by ¹H NMR spectroscopy. [b] Ae = 40 μmol, [D₆]benzene = 0.4 mL. [c] Ae = 20 μmol, [D₆]benzene = 0.4 mL.

Scheme 2. Common insertion mechanism for cyclohydroamination reactions.^[2]

Ca > Sr ≫ Ba; that is, it was the exact opposite of that observed during intermolecular hydroamination and hydrophosphination reactions catalyzed by these three complexes.^[24] The low catalytic activity exhibited by **3** toward the reactive substrate **A** under the chosen experimental conditions was in agreement with another experiment that utilized (**6**)₂ (Table 1, entry 4) as the catalytic precursor, which gave a comparable result. Note that Hill and co-workers reported failed attempts to catalyze the cyclohydroamination of **A** with [Ba{N(SiMe₃)₂}₂], [Ba{N(SiMe₃)₂}(thf)₂], or [Ba{CH(SiMe₃)₂}(thf)]^[9g].

The reaction rates were somewhat lower in the case of **B**, which allowed a more accurate screening of the catalyst efficiency, and we therefore focused more closely on this substrate. The purity of **B** was regularly checked by employing [(BDI)CaN(SiMe₃)₂(thf)], for which the reaction rates at 60 °C were too fast to be determined accurately (Table 1, entry 5). Hill and co-workers reported full conversion of **B** (and **A**) within 15 min with this catalyst ([Ca]₀/[substrate]₀ = 1:10) at room temperature,^[8] and similar results were obtained in our hands. Full conversion required 1.5 and 5 h, respectively, with the Ca and Sr catalysts **1** and **2** (Table 1, entries 6 and 7), thus affording 2,4,4-trimethylpyrrolidine selectively. Again, the Ba catalyst **3** was much less efficient (Table 1, entry 8). Besides, the conversion of 12 equivalents of **B** versus the catalyst **1–3** was monitored by ¹H NMR spectroscopy.^[30] Complete conversion was achieved in 20 and 60 min with **1** and **2**, respectively; in contrast, only 28% of **B** was converted after 60 min when **3** was employed. This outcome further corroborated the activity trend Ca > Sr > Ba for these alkaline-earth metal catalysts incorporating N(SiMe₃)₂⁻ moieties. The fact that this trend depends on the nature of the metal and not amide group was demonstrated when catalysts bearing the N(SiMe₂H)₂⁻ amide were tested. The Sr catalyst (**5**)₂ proved noticeably more efficient than its Ba derivative (**6**)₂ (compare entries 11 and 12 in Table 1).

The Ca complex **4** was less efficient than its Sr analogue (**5**)₂ (Table 1, entries 10 and 11), but this seemingly contradictory result was later explained when a specific and preponderant decomposition pathway was identified for catalyst **4** (see below). To remove any potential ambiguity, the β-diketiminate complexes **11–13** were also tested, with catalytic performances decreasing steadily according to Ca > Sr > Ba (Table 1, entries 18–20).

Although it does not affect the overall Ca > Sr ≫ Ba trend, the nature of the amide group on the metal center bears a strong influence on the outcome of catalytic reactions. Independently of the nature of the metal center and ancillary ligand, slower rates were observed with the N(SiMe₂H)₂⁻ group bound to the metal center than with the N(SiMe₃)₂⁻ group. In the case of the Ca catalysts, this was particularly obvious upon comparison of entries 6 and 9, entries 13 and 14 (taking place at 60 and 80 °C, respectively), or even entries 5 and 18 in Table 1. The superiority of the Ae–N(SiMe₃)₂ species in terms of activity was also evidenced for Sr (Table 1, entries 7 and 11) and Ba complexes (Table 1, entries 8 and 12). These findings could be easily rationalized on the basis of the relative acidity of the HN(SiMe₂H)₂ and HN(SiMe₃)₂ moieties (pK_a = 22.6 and 25.8, respectively).^[31] Indeed, Hill and co-workers have elegantly demonstrated the reversibility of the protonolysis of [(BDI)CaN(SiMe₃)₂(thf)] with benzylamine,^[32] and have shown that a similar equilibrium constituted a serious impediment to fast catalytic turnovers in the case of HN(SiMe₃)₂ released upon the addition of an excess of substrate **B** to [(BDI)CaN(SiMe₃)₂(thf)]. In contrast, the cyclohydroamination of **B** catalyzed by [(BDI)MgMe(thf)] was not hindered by the formation of CH₄.^[9c,g] Hence, the initial equilibrium between the catalyst [(LX)AeN(SiMe₂R)₂(thf)_x] and the active species (Scheme 2) lies much more toward the side of the reactants with the relatively acidic HN(SiMe₂H)₂ moiety (R = H) than it does for the HN(SiMe₃)₂ species (R = Me), thus resulting in lower catalytic turnover rates. The higher catalytic initiation efficiency of Group 3 metal–N(SiMe₃)₂ complexes over their –N(SiHMe₂)₂ analogues in cyclohydroamination has been reported also by O’Shaughnessy and Scott^[33] and Hultsch and Hampel.^[34] Besides, a deactivation pathway specific to [(LX)AeN(SiMe₂H)₂(thf)_x] complexes was discovered, with ensuing limited turnover numbers and lower reaction rates (see below).

The influence of the ligand scaffold was interrogated by utilizing Ca complexes only. Comparative tests performed under rigorously identical conditions revealed that for the

complete family of $[(LO^{\delta})CaN(SiMe_2H)_2(thf)_x]$ catalysts ($i=1-4$)^[35,36] the activity varied according to $9 < 4 < 8 < (7)_2$ (Table 1, entries 14–17); that is, the activity essentially decreased when the number of donor atoms increased in the supporting ligand. Decreasing hydroamination activity with increasing electron-donating and chelating ability of the ancillary ligand had been postulated before,^[12a] but to the best of our knowledge it has been demonstrated here for the first time with a family of directly comparable Ca catalysts that differ only in the nature of the phenolate ligand. However, note that Hill and co-workers reported that the unsolvated complexes $[Ae\{N(SiMe_3)_2\}_2]$ were generally less efficient than their THF-bound analogues $[Ae\{N(SiMe_3)_2\}_2(thf)_2]$ ($Ae=Mg, Ca, Sr$). Our interpretation of these and our results is that low coordination number and chelating ability are intrinsically beneficial to catalytic activity provided it does not come at the expense of catalyst stability. Interestingly, the four-coordinated Ca complex **11** was slightly less active than $(7)_2$ (Table 1, entries 14 and 18), thus indicating that extrapolation of these preliminary conclusions across different families of ligands may be premature. The limited synthetic availability of $[(LO^{\delta})CaN(SiMe_3)_2(thf)_x]$ catalysts (stable only for $i=1$ and 4) did not allow the analogous comparison with $[(BDI)CaN(SiMe_3)_2(thf)]$.

On the whole, the cyclization of **A** and **B** is substantially slower with **1–3** than with $[(BDI)CaN(SiMe_3)_2(thf)]$.^[9] Nonetheless, reaction rates for Ca–phenolate systems, in particular $(10)_2$ and $(7)_2$ (Table 1, entries 13 and 14), compare favorably with those reported by Roesky and co-workers for aminotroponimate^[13] and 2,5-bis[*N*-(aryl)iminomethyl]pyrrolyl^[14] Ca and Sr catalysts. The Ca complexes developed by Wixey and Ward supported by chiral 1,2-diamines^[15] or bisimidazoline^[16] ligands are even less active, although they afford the formation of the cyclic products with some degree of enantioselectivity (i.e., 5–26% *ee*).

Kinetic studies: The conversion of 12 equivalents of **B** catalyzed by the aminophenolate complexes **1–3** and the β -diketiminate complexes **11–13** was monitored by ¹H NMR spectroscopy to gain further information on the influence of the metal center (Table 2).^[30] The semilogarithmic plots of substrate conversion versus reaction gave straight lines in all cases, thus indicating first-order dependence upon monomer concentration (Figures 4 and 5). The observed rate constants

Table 2. Cyclohydroamination of aminoalkene **B** catalyzed by **1–4** and **11–13**.^[a]

Entry	Catalyst	<i>t</i> [h]	Conv. ^[b] [%]	<i>k</i> _{obs} [10 ^{−4} s ^{−1}]	
1	$[(LO^{\delta})CaN(SiMe_3)_2]$	1	0.3	95	24.0
2	$[(LO^{\delta})SrN(SiMe_3)_2(thf)]$	2	1	93	7.4
3	$[(LO^{\delta})BaN(SiMe_3)_2]$	3	1	28	1.0
4	$[(BDI)CaN(SiMe_2H)_2(thf)]$	11	0.75	93	10.3
5	$[(BDI)SrN(SiMe_2H)_2(thf)_2]$	12	3	91	2.6
6	$[(BDI)BaN(SiMe_2H)_2(thf)_2]$	13	8	89	0.9
7	$[(LO^{\delta})CaN(SiMe_2H)_2(thf)]$	4	29	92	0.1

[a] $Ae=20 \mu mol$, 80 °C, $[D_6]benzene=0.4 mL$. [b] Conversion determined by ¹H NMR spectroscopy.

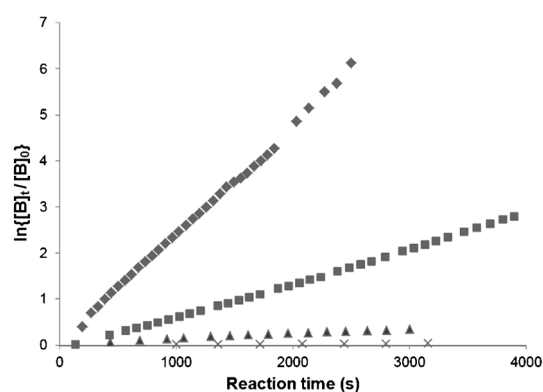


Figure 4. Semilogarithmic plot of substrate conversion versus reaction time for the cyclohydroamination of **B** (12 equiv vs. Ae , 20 μmol of Ae) catalyzed by $[(LO^{\delta})CaN(SiMe_3)_2]$ (**1**, $k_{obs}=24.0 \times 10^{-4} s^{-1}$; \blacklozenge), $[(LO^{\delta})SrN(SiMe_3)_2(thf)]$ (**2**, $k_{obs}=7.4 \times 10^{-4} s^{-1}$; \blacksquare), $[(LO^{\delta})BaN(SiMe_3)_2]$ (**3**, $k_{obs}=1.0 \times 10^{-4} s^{-1}$; \blacktriangle), and $[(LO^{\delta})CaN(SiMe_2H)_2(thf)]$ (**4**, $k_{obs}=0.1 \times 10^{-4} s^{-1}$; \times) in $[D_6]benzene$ (0.4 mL) at 80 °C.

k_{obs} for the Ca, Sr, and Ba (**1–3**) aminophenolate catalysts were 24.0×10^{-4} , 7.4×10^{-4} , and $1.0 \times 10^{-4} s^{-1}$, respectively. It is not clear whether the role of the coordinated molecule of THF in **2** is neutral or prejudicial to the activity of the catalyst; however, this possibility could not be assessed because,

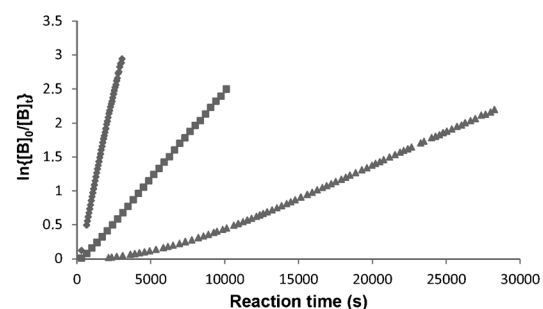


Figure 5. Semilogarithmic plot of substrate conversion versus reaction time for the cyclohydroamination of **B** (12 equiv vs. Ae , 20 μmol of Ae) catalyzed by $[(BDI)CaN(SiMe_2H)_2(thf)]$ (**11**, $k_{obs}=10.3 \times 10^{-4} s^{-1}$; \blacklozenge), $[(BDI)SrN(SiMe_2H)_2(thf)_2]$ (**12**, $k_{obs}=2.6 \times 10^{-4} s^{-1}$; \blacksquare), and $[(BDI)BaN(SiMe_2H)_2(thf)_2]$ (**13**, $k_{obs}=0.9 \times 10^{-4} s^{-1}$; \blacktriangle) in $[D_6]benzene$ (0.4 mL) at 80 °C.

despite our repeated synthetic efforts, this single THF molecule could not be removed from the metal center. The reactions proceeded more slowly with the catalysts **11–13** containing the β -diketiminate scaffold ($k_{obs}=10.3 \times 10^{-4}$, 2.6×10^{-4} , and $0.9 \times 10^{-4} s^{-1}$, respectively; Table 2). Comparison across the two families are ill advised as both the ligand and amide groups differ from one to the other family; yet, for both families, these data fully agree with the trend $Ca > Sr \gg Ba$ observed earlier. Although the cyclization of only 12 equivalents of **B** with **3** or **13** is relatively slow, these constitute the first examples of Ba catalysts for cyclohydroamination. Catalyst **4**, with its $N(SiMe_2H)^-$ amide group, also exhibited a partial kinetic order of one in substrate concen-

tration, but as expected on the basis of the preliminary test it unveiled very low catalytic efficiency in comparison with **1** (Table 2, entries 1 and 7), with a k_{obs} value of $0.1 \times 10^{-4} \text{ s}^{-1}$ only.

The situation was different with (**7**)₂ and **8**, that is, the catalysts that had displayed the best performances in the series [(LO¹)AeN(SiMe₂H)₂(thf)_x] during the qualitative tests.^[37] The situation of (**7**)₂ was envisaged in the light of previous studies by pulse-gradient spin echo NMR spectroscopy,^[22n] which showed that (**7**)₂ fully dissociates in [D₆]benzene. It seemed pertinent to consider that this would also be the case in the additional presence of 12 equivalents of substrate (versus Ca), and therefore we consider that the cyclohydroamination catalyst in this case is the monomeric **7**.^[35] After, respectively, a short or rather long (ca. 2 or 40 min) induction period, the cyclization of **B** increased linearly with reaction time for both **7** and **8**, thus indicating a zero-order dependence upon [B]₀.^[26] Further studies were undertaken with **7**, the most efficient of these two catalysts, to keep reaction times reasonably short and compatible with ¹H NMR spectroscopic monitoring. The reactions were performed at 80 °C by maintaining the concentration in **7** constant (50.0 mM), but with varying substrate concentration in the range 0.5–4.0 M (Figure 6). In all cases, an initial curvature

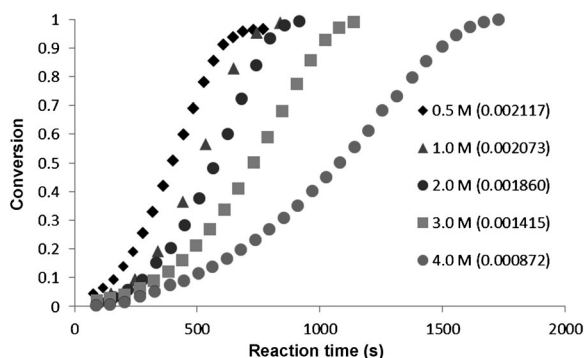


Figure 6. Plot of substrate conversion versus reaction time for the cyclohydroamination of **B** catalyzed by [(LO¹)CaN(SiMe₂H)₂] (**7**) at 80 °C with constant initial concentration of **7** (50.0 mM) and [B]₀ = 0.5 M ($k_{\text{obs}} = 21.1 \times 10^{-4} \text{ mol s}^{-1}$; ◆), 1.0 M ($k_{\text{obs}} = 20.7 \times 10^{-4} \text{ mol s}^{-1}$; ▲), 2.0 M ($k_{\text{obs}} = 18.6 \times 10^{-4} \text{ mol s}^{-1}$; ●), 3.0 M ($k_{\text{obs}} = 14.1 \times 10^{-4} \text{ mol s}^{-1}$; ■), and 4.0 M ($k_{\text{obs}} = 8.7 \times 10^{-4} \text{ mol s}^{-1}$; ●).

indicative of rate acceleration was observed and became more pronounced with increasing substrate concentration. Moreover, after this induction period, the formation of 2-methyl-4,4-diphenylpyrrolidine increased linearly with reaction time up to approximately 90–95% conversion (i.e., until inhibition by reversible coordination of the product), thus confirming a 0th order in [B]₀. This outcome is compatible with the generally accepted mechanism for the cyclohydroamination reaction, in which the rate-determining step consists of the insertion of the polarized coordinated olefin into the Ae–N bond (Scheme 2). Finally, the k_{obs} value decreased markedly with increasing initial substrate concentration, from $k_{\text{obs}} = 21.2 \times 10^{-4} \text{ mol s}^{-1}$ for [B]₀ = 0.50 M down to

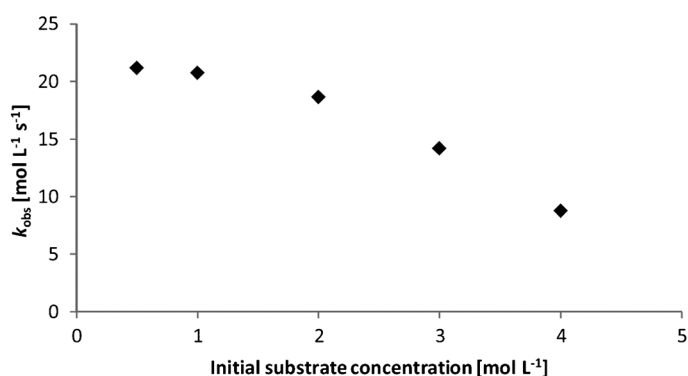


Figure 7. Plot of k_{obs} values versus [B]₀ for the cyclohydroamination of **B** catalyzed by [(LO¹)CaN(SiMe₂H)₂] (**7**) at 80 °C with [7]₀ = 50.0 mM and [B]₀ = 0.5–4.0 M.

$8.7 \times 10^{-4} \text{ mol s}^{-1}$ for [B]₀ = 4.0 M (Figure 7). These results were diagnostic of catalyst inhibition by the substrate; a similar phenomenon has already been documented by Hultzsich and co-workers for the cyclohydroamination of 1-amino-4-pentene catalyzed by chiral binaphtholate lanthanide catalysts.^[4p]

The rate dependence upon catalyst concentration was examined by varying the initial concentration of **7** in the range 4.30–52.9 mM while keeping [B]₀ constant (0.60 M). The values of k_{obs} extracted from the linear regime (substrate conversion in the range 30–90%) of the plot of conversion versus reaction time for each catalyst concentration from 1.5×10^{-4} to $21.2 \times 10^{-4} \text{ mol L}^{-1} \text{ s}^{-1}$. The plot of k_{obs} value versus the initial concentration of the catalyst was a straight line (Figure 8), and the corresponding plot of $\ln(k_{\text{obs}})$ versus $\ln([7]_0)$ was a line with the slope of 1.06 ($R^2 = 0.9969$).^[26] Both of these findings were diagnostic of a first-order dependence upon catalyst concentration, thus confirming that (**7**)₂ did not preserve its dimeric nature under catalytic conditions, as otherwise a noninteger kinetic order of 0.5 in catalyst concentration typical of dimeric precatalysts would have been expected.^[38] Under the assumption that (**7**)₂ fully dissociates in solution, the cyclization of **B** catalyzed by **7**

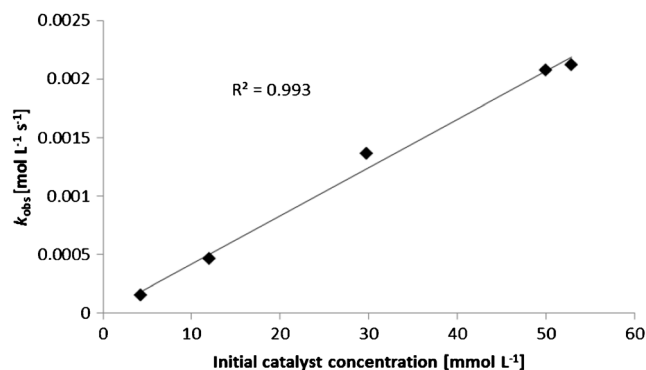


Figure 8. Plot of k_{obs} values versus initial catalyst concentration for the cyclohydroamination of **B** catalyzed by [(LO¹)CaN(SiMe₂H)₂] (**7**) in [D₆]benzene at 80 °C with [B]₀ = 0.6 M.

therefore obeyed the empirically determined rate law given in Equation (1):

$$-d[\mathbf{B}]/dt = k[\mathbf{7}]_0 \quad (1)$$

The activation energy for the cyclohydroamination of **B** catalyzed by **7** was $E_a = 97.6 \text{ kJ mol}^{-1}$ according to Arrhenius analysis of values of k_{obs} determined in the temperature range 313–353 K.^[26] The corresponding activation enthalpy ($\Delta H^\ddagger = 94.9(3.0) \text{ kJ mol}^{-1}$) and activation entropy ($\Delta S^\ddagger = -29.7(8.9) \text{ J mol}^{-1} \text{ K}^{-1}$) were determined by using Eyring analysis. These values differ largely from those reported by Hill and co-workers for the cyclization of (1-allylcyclohexyl)amine (a substrate considerably easier to cyclize than **B**) with $[(\text{BDI})\text{CaN}(\text{SiMe}_3)_2(\text{thf})]$ ($\Delta H^\ddagger = 63.1 \text{ kJ mol}^{-1}$ and $\Delta S^\ddagger = -77.7 \text{ J mol}^{-1} \text{ K}^{-1}$).^[9g]

The initial qualitative screening suggested that $[(\text{LO}^1)\text{CaN}(\text{SiMe}_3)_2]$ (**(10)**₂) displays greater efficacy than its $[(\text{LO}^1)\text{CaN}(\text{SiMe}_2\text{H})_2]$ congener (**(7)**₂) (Table 1, entries 13 and 14). The behavior of **(10)**₂ toward substrate **B** was investigated in more detail (12 equiv of **B** vs. Ca). The cyclization occurred at 80 °C with zero-order dependence upon $[\mathbf{B}]_0$, but without an induction period and no sign of inhibition by the substrate or product (Figure 9). The activation energy ($E_a = 85.0 \text{ kJ mol}^{-1}$) and activation enthalpy and entropy ($\Delta H^\ddagger = 82.4(4.1) \text{ kJ mol}^{-1}$ and $\Delta S^\ddagger = -41.3(13.1) \text{ J mol}^{-1} \text{ K}^{-1}$) deduced from analyses of the Arrhenius and Eyring ($R^2 = 0.9926$ and 0.9920 , respectively) plots^[26] were markedly lower than those determined for **(7)**₂.

Stoichiometric and model reactions: In an effort to gain insight into the mechanisms that operate with our Ae-phenolate cyclohydroamination catalysts, the stoichiometric reaction of $[(\text{LO}^4)\text{CaN}(\text{SiMe}_3)_2]$ (**1**) and aminoalkene **B** in $[\text{D}_6]\text{benzene}$ was monitored by ¹H NMR spectroscopy.^[26] No sign of evolution at room temperature was noted after 30 min. A very slow formation of 2,4,4-trimethylpyrrolidine at 40 °C was detected, and only 59% of the substrate had been converted after 90 minutes. Formation of the cyclic amine product was concomitant with the disappearance of **B** (Figure 10), and the associated semi-logarithmic plot of the consumption of **B** versus the reaction time was linear, consistent with first-order dependence on $[\mathbf{B}]_0$.

During the course of 90 min, only incremental amounts of free $\text{HN}(\text{SiMe}_3)_2$ (no more than 2% with respect to Ca or **B**) were detected at any given time, and in particular the quantity of free amine was far below that expected from aminolysis of the $\text{Ca}-\text{N}(\text{SiMe}_3)_2$ bond by $\text{H}_2\text{NCH}_2\text{C}(\text{CH}_3)_2\text{CH}_2\text{CH}=\text{CH}_2$. Moreover, no resonance signals for the phenoxy species other than those for starting **1** were detected. Similar observations have been made previously by Hill and co-workers with $[(\text{BDI})\text{CaN}(\text{SiMe}_3)_2(\text{thf})]$, and indeed we have checked that under our experimental protocol no

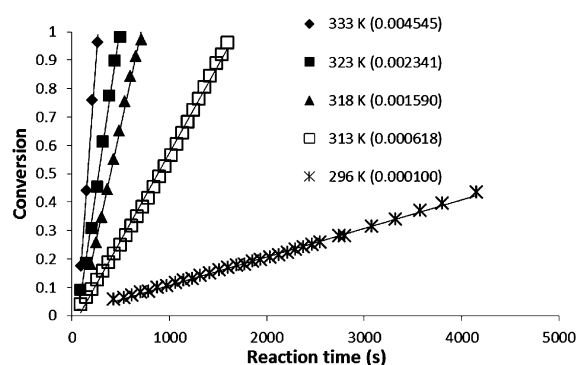
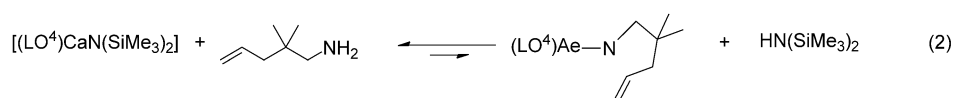


Figure 9. Plots of substrate conversion versus reaction time for the cyclohydroamination of **B** catalyzed by $[(\text{LO}^1)\text{CaN}(\text{SiMe}_3)_2]$ (**(10)**₂) ($[(\mathbf{10})_2] = 10 \mu\text{mol}$; 12 equiv of **B** versus Ca; $[\text{D}_6]\text{benzene} = 0.4 \text{ mL}$) at 296, 313, 318, 323, and 333 K.

obvious change in the resonance signals characteristic of the Ca complex were noted upon addition of one, or even four, equivalents of **B** to $[(\text{BDI})\text{CaN}(\text{SiMe}_3)_2(\text{thf})]$; in both cases, **B** was fully cyclized within 10 minutes at room temperature.^[26] Whether with this complex or with **1**, the presence of a resonance at very high field (typically between $\delta = -0.30$ and -1.90 ppm), indicative of $\text{Ca}-\text{NHR}$, moieties was never discovered. Besides, signs for the presence of other short-lived species, such as those that result from the insertion of the polarized $\text{C}=\text{C}$ unsaturation into the $(\text{LO}^4)\text{Ca}-\text{NHR}$ bond, were not detectable on the NMR timescale. These observations suggest that the reaction between **1** and **B** is an acid–base equilibrium with a strong preference for the side of the reactants [Eq. (2)] and that $[(\text{LO}^4)\text{CaN}(\text{SiMe}_3)_2]$ probably constitutes the main catalyst resting state in the catalytic cycle associated with **1**.

To enhance our understanding of the behavior of complexes that contain the $\text{N}(\text{SiMe}_2\text{H})_2^-$ amido group, the reaction of $[(\text{LO}^4)\text{CaN}(\text{SiMe}_2\text{H})_2(\text{thf})]$ (**4**) with one equivalent



of **B** in $[\text{D}_6]\text{benzene}$ was monitored in the same fashion by variable-temperature (VT) ¹H NMR spectroscopy (Figure 11). The system was essentially inert below 60 °C, as no evolution was noted over 1–2 h. New resonance signals were detected at 60 °C, notably at $\delta = 4.47$ and 2.74 ppm; yet, their intensities were rather low, and these signals did not match those expected for 2,4,4-trimethylpyrrolidine. The cyclization of **B** took place slowly at 80 °C and several sets of signals were detected, which clearly identified as corresponding to the expected cyclic amine product (thus indicating less than 10% conversion of the substrate after 50 minutes at 80 °C). Signals of the aforementioned species at $\delta = 4.47$ and 2.74 ppm, for which the intensities had substantially enhanced, were also detected. Besides, these signals were

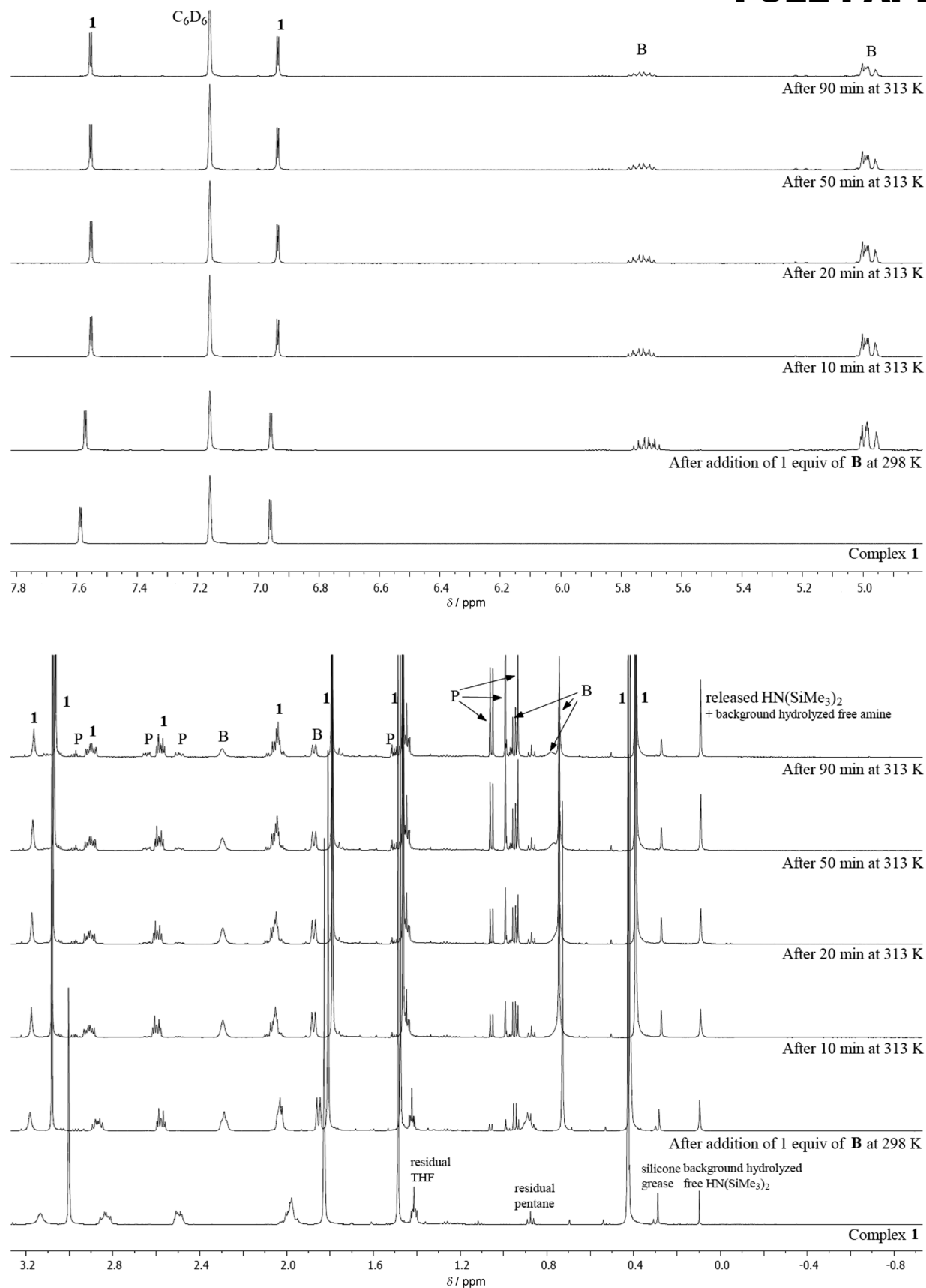


Figure 10. VT ¹H NMR (500.1 MHz, [D₆]benzene) monitoring of the reaction of [(LO⁺)CaN(SiMe₃)₂] (**1**) and one equivalent of **B** (**1** = 40 μmol, [D₆]benzene = 0.4 mL). Top: δ = 4.9–7.8 ppm; bottom: δ = -0.9–3.2 ppm. Resonance signals that belong to the catalyst, substrate, and cyclized product are identified by **1**, **B**, and **P**, respectively. Note the formation of a small amount of HN(SiMe₃)₂ in the spectrum of complex **1** by itself. The integration of this background amine was subtracted for calculations of HN(SiMe₃)₂ released upon reaction of **1** with **B**.

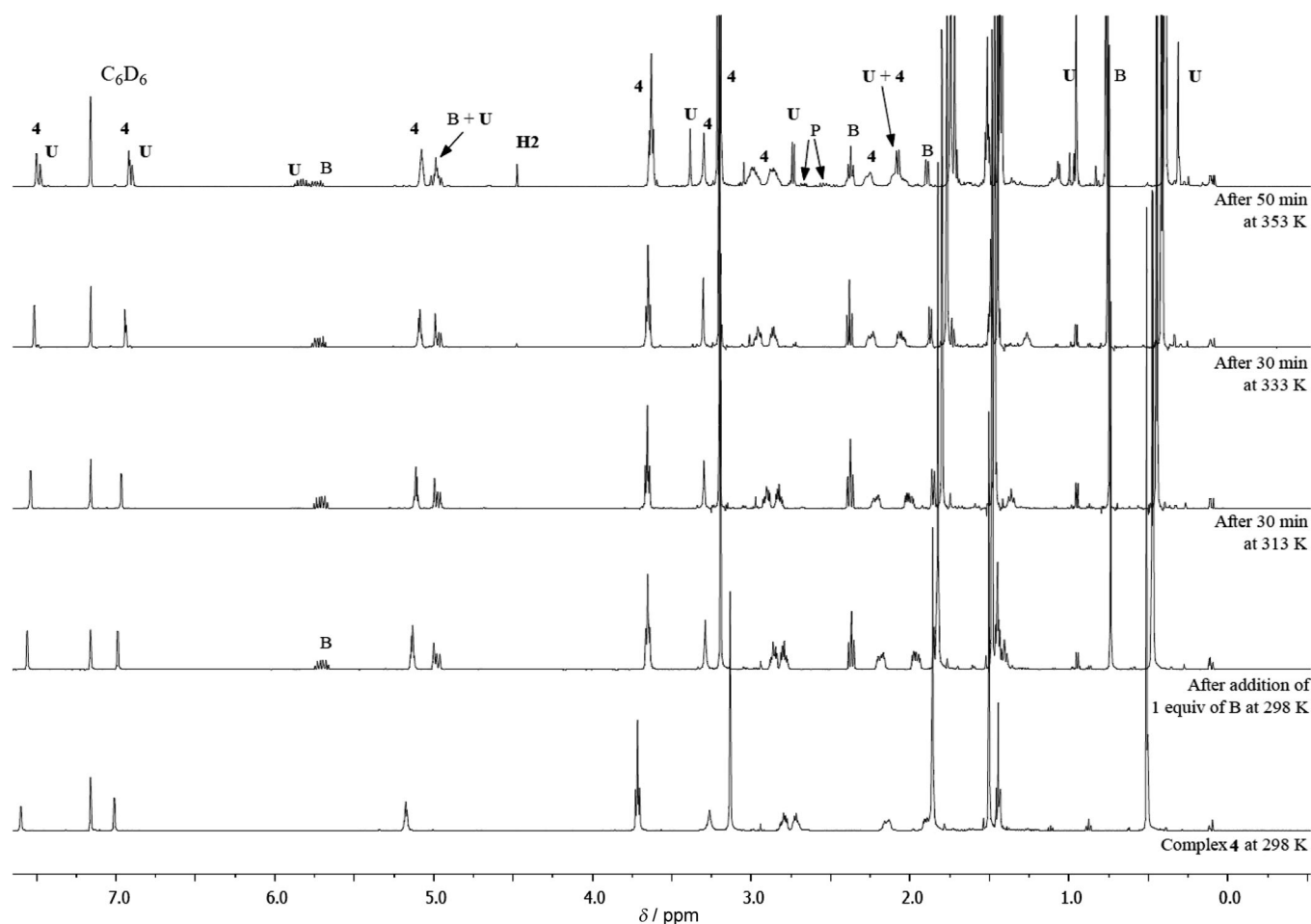


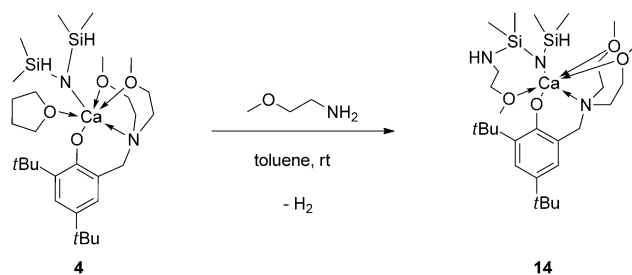
Figure 11. VT ^1H NMR (500.1 MHz, $[\text{D}_6]$ benzene) monitoring of the reaction of $[(\text{LO}^4)\text{CaN}(\text{SiMe}_2\text{H})_2(\text{thf})]$ (**4**) and one equivalent of aminoalkene **B** (**4** = 40 μmol , $[\text{D}_6]$ benzene = 0.4 mL). Resonance signals that belong to **4**, substrate, cyclic product, dihydrogen, and the unidentified byproducts are identified by **4**, **B**, **P**, **H₂**, and **U**, respectively.

accompanied by new signals of strong intensities at $\delta = 7.48$, 6.90, and 0.90 ppm, whereas another signal characteristic of the Me_2SiH moiety was identified at $\delta = 5.02$ ppm (and overlapped partly with the vinylic resonance of **B**). These observations unambiguously suggested that **4** did not remain intact during the reaction, but a new metallic species (**U**) formed in large proportions. Attempts to identify these byproducts at this stage were hampered by the reactivity of **B** toward **4**, and also potentially toward this new metallic species, and by the complexity of the ^1H NMR data in the region $\delta = 0.0$ –4.0 ppm.

The stoichiometric reaction of **4** and 2-methoxyethylamine, carried out on a preparative scale and also monitored by ^1H NMR spectroscopy, was most informative. Hill and co-workers had previously shown that the reaction of $[(\text{BDI})\text{CaN}(\text{SiMe}_3)_2(\text{thf})]$ and 2-methoxyethylamine yielded the dimeric $[(\text{BDI})\text{Ca}\{\mu\text{-NH}(\text{CH}_2)_2\text{OMe}\}_2]$ in good yields,^[39] whereas with its Sr parent the amine adduct $[(\text{BDI})\text{SrN}(\text{SiMe}_3)_2\{\text{H}_2\text{N}(\text{CH}_2)_2\text{OMe}\}]$ was obtained preponderantly.^[9e] To our surprise, we found that the equimolar reaction of **4** and 2-methoxyethylamine at room temperature

did not afford either of the potentially expected complexes, but yielded instead $[(\text{LO}^4)\text{CaN}(\text{SiMe}_2\text{H})(\text{SiMe}_2\text{NH-CH}_2\text{CH}_2\text{OCH}_3)]$ (**14**) as a crystalline colorless solid (the nonoptimized yield was 31 %) following fractionated recrystallization (Scheme 3).

The ^1H NMR spectrum of **14** is characterized by two doublets at $\delta = 7.57$ and 7.02 ppm that correspond to the aromatic hydrogen atoms ($^4J_{\text{H-H}} = 2.8$ Hz), a multiplet at $\delta = 5.09$ ppm assigned to SiH ($^1J_{\text{Si-H}} = 172$ Hz); the resonance



Scheme 3. Reaction of **4** and 2-methoxyethylamine to yield **14**.

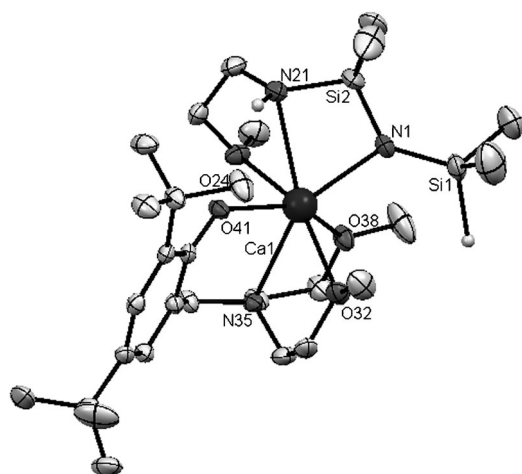


Figure 12. Solid-state structure of $[(\text{LO}^4)\text{CaN}(\text{SiMe}_2\text{H})(\text{SiMe}_2\text{NHCH}_2\text{CH}_2\text{OMe})]$ (**14**). The noninteracting solvent molecule and hydrogen atoms (except those on N and Si atoms) are omitted for clarity. Ellipsoids are drawn at the 50% probability level. Selected bond lengths [Å] and angles [°]: N1–Ca1 2.389(2), N21–Ca1 2.692(2), O24–Ca1 2.504(2), O32–Ca1 2.466(2), N35–Ca1 2.565(2), O38–Ca1 2.463(2), O41–Ca1 2.241(1), N1–Si:2 1.677(2), N21–Si2 1.758(2); N1–Si2–N21 105.74(9), Si2–N1–Si1 130.4(1).

signals for the $\text{NSi}(\text{CH}_3)_2\text{NH}$ and $\text{NSi}(\text{CH}_3)_2\text{H}$ moieties are found as a doublet and singlet at $\delta = 0.38$ ($^3J_{\text{H-H}} = 2.8$ Hz) and 0.33 ppm, respectively.^[26] By combining the ^1H , $\{^1\text{H}\}^{13}\text{C}$, and HMBC NMR spectroscopic data, and by analogy with related reported examples,^[40] a triplet in the ^1H NMR spectrum at $\delta = 0.92$ ppm with integration for 1H was assigned to the amine SiNHCH_2 . The $\{^1\text{H}\}^{29}\text{Si}$ NMR spectrum of **14** exhibited two singlets at $\delta = -13.25$ and -30.06 ppm, indicative of two nonequivalent silylamido groups. The solid-state structure of **14** was determined by X-ray diffraction studies of crystals obtained from a solution in pentane (Figure 12). The Ca atom is seven-coordinated. The Ca1–N21 bond length (2.69 Å) is longer than for Ca1–N1 (2.39 Å) and Ca1–N35 (2.56 Å), which are nearly equivalent to those found in $[(\text{LO}^6)\text{CaN}(\text{SiMe}_2\text{H})_2(\text{thf})]$ (**4**). The Si2–N21 bond length of 1.76 Å is markedly longer than for Si2–N1 (1.68 Å). The Si2–N1–Si1 angle of 130.3° in **14** is a little wider than in its parent compound **4** (125.1°).^[22n]

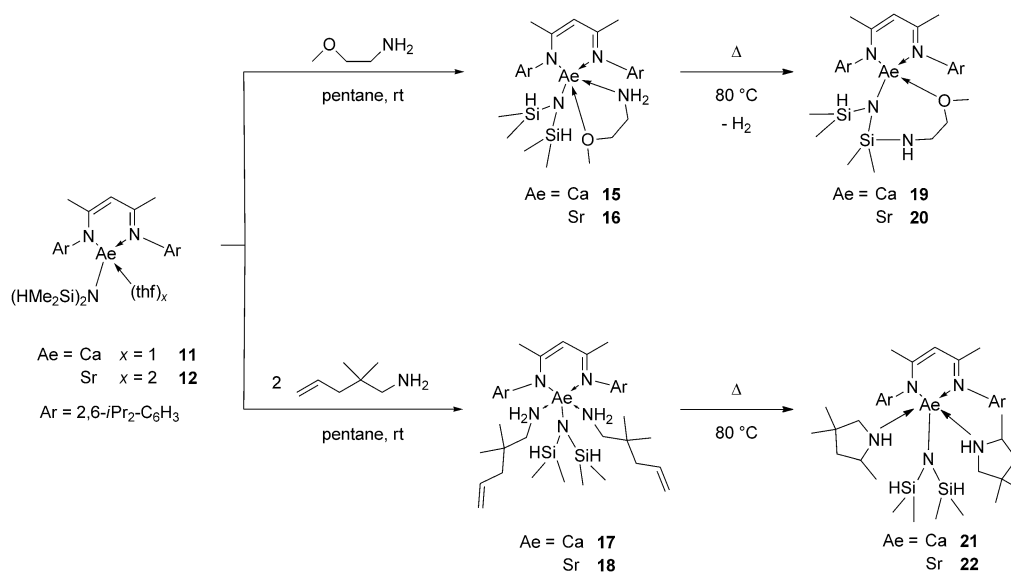
The formation for **14** is reminiscent of the cross-dehydrocoupling of organosilanes with amines mediated by a tris(oxazolonyl)boratomagnesium amide precatalyst reported recently by Sadow and co-workers.^[41] Indeed, the ^1H NMR spectroscopic monitoring of the equimolar reaction of **4** and 2-methoxyethylamine in $[\text{D}_6]$ benzene at room temperature indicated gradual, but eventually the near-complete (after 12 h) consumption of **4** to give predominately **14** with the release of large amounts of H_2 (singlet at $\delta = 4.47$ ppm), small contamination with $[(\text{LO}^4)_2\text{Ca}]$, negligible amounts of free $\text{HN}(\text{SiMe}_2\text{H})_2$ (doublet at $\delta = 0.11$ ppm, $^3J_{\text{H-H}} = 3.1$ Hz; multiplet at $\delta = 4.71$ ppm), and an unidentified $[(\text{LX})\text{Ca-NHR}]$ species (broad singlet at $\delta = -0.72$ ppm) were also discerned.^[26]

The key ^1H NMR data for **14** were fully consistent with the new species **U** formed (along with H_2) during the reaction of the Ca–aminophenolate **4** and one equivalent of **B** (see above; Figure 11). We therefore concluded that a complex of the type $[(\text{LO}^4)\text{CaN}(\text{SiMe}_2\text{H})\{\text{SiMe}_2\text{NHCH}_2\text{C}(\text{CH}_3)_2\text{CH}_2\text{CH}=\text{CH}_2\}]$ was the main product of decomposition (i.e., **U**) detected during the cyclohydroamination of **B**. No information regarding the catalytic ability toward the cyclohydroamination of such a complex was directly gathered. However, we verified that **14** was itself totally inert toward **B**, even at 80°C . One can therefore postulate that $[(\text{LO}^4)\text{CaN}(\text{SiMe}_2\text{H})\{\text{SiMe}_2\text{NHCH}_2\text{C}(\text{CH}_3)_2\text{CH}_2\text{CH}=\text{CH}_2\}]$ (**U**) is catalytically inactive and that its rapid formation under catalytic conditions results in lower reactions rates and turnover numbers.

The reaction of $[(\text{BDI})\text{CaN}(\text{SiMe}_2\text{H})_2(\text{thf})]$ (**11**) with **B** in $[\text{D}_6]$ benzene monitored by VT ^1H NMR spectroscopy demonstrated that the deactivation pathway identified in the case of **4** does not necessarily occur with all $[(\text{LX})\text{CaN}(\text{SiMe}_2\text{H})_2(\text{thf})_x]$, at least at the temperatures at which these compounds are catalytically active for cyclohydroamination. Whether with 1 or 12 equivalents of **B** versus **11**, the formation of 2,4,4-trimethylpyrrolidine proceeded extremely slowly at room temperature (16% conversion of one equivalent of **B** after 60 minutes), whereas clean cyclization without the formation of byproducts occurred more rapidly at 60°C (22% conversion of 12 equivalents of **B** after 75 min). The formation of H_2 and species of the type “ $[(\text{BDI})\text{CaN}(\text{SiMe}_2\text{H})\{\text{SiMe}_2\text{NHCH}_2\text{C}(\text{CH}_3)_2\text{CH}_2\text{CH}=\text{CH}_2\}(\text{thf})_x]$ ” ($x = 0$ or 1) was never detected at these temperatures (20 – 60°C). These observations led to the clean and quantitative preparations of the model compounds $[(\text{BDI})\text{AeN}(\text{SiMe}_2\text{H})_2\{\text{H}_2\text{N}(\text{CH}_2)_2\text{OMe}\}]$ ($\text{Ae} = \text{Ca}$ (**15**); Sr (**16**)) and $[(\text{BDI})\text{AeN}(\text{SiMe}_2\text{H})_2\{\text{H}_2\text{NCH}_2\text{C}(\text{CH}_3)_2\text{CH}_2\text{CH}=\text{CH}_2\}]$ ($\text{Ae} = \text{Ca}$ (**17**), Sr (**18**)) by treatment of **11** or **12** with the appropriate amine, 2-methoxyethylamine, or **B** in pentane at room temperature (Scheme 4).

However, although complexes **15** and **16** were perfectly stable in solution up to 60°C according to VT ^1H NMR spectroscopy, they evolved at 80°C over two hours to give the complexes $[(\text{BDI})\text{AeN}(\text{SiMe}_2\text{H})\{\text{SiMe}_2\text{HN}(\text{CH}_2)_2\text{OMe}\}]$ ($\text{Ae} = \text{Ca}$ (**19**), Sr (**20**)) almost quantitatively with the release of H_2 . The Sr complex **16** was similar to its $[(\text{BDI})\text{SrN}(\text{SiMe}_3)_2\{\text{H}_2\text{N}(\text{CH}_2)_2\text{OMe}\}]$ analogue already described by Hill and co-workers.^[9g] In particular, the ^1H NMR spectrum of **16** exhibited a triplet at $\delta = 0.04$ ppm assigned to the hydrogen atoms of the coordinated chelating amine $\text{H}_2\text{N}(\text{CH}_2)_2\text{OMe}$, whereas the corresponding resonance was located at $\delta = -0.09$ ppm in $[(\text{BDI})\text{SrN}(\text{SiMe}_3)_2\{\text{H}_2\text{N}(\text{CH}_2)_2\text{OMe}\}]$.^[42]

The excellent stability of **15** and **16** in solution at room temperature combined with the inability of **11** and **12** to mediate the cyclization of **B** below 60 – 80°C prompted us to synthesize model compounds by reaction of **11** or **12** with **B** on a preparative scale. Reactions in pentane at 25°C afforded $[(\text{BDI})\text{AeN}(\text{SiMe}_2\text{H})_2\{\text{H}_2\text{NCH}_2\text{C}(\text{CH}_3)_2\text{CH}_2\text{CH}=\text{CH}_2\}]_2$ ($\text{Ae} = \text{Ca}$ (**17**), Sr (**18**)) as pale yellow solids in excellent



Scheme 4. Preparation of the model compounds **15–22**.

yields (Scheme 4). The identities of these compounds were confirmed by NMR and FTIR spectroscopy, and their purities were attested by combustion analysis. Notably, in the ^1H NMR spectra recorded in $[\text{D}_6]$ benzene, the broad resonance for the H_2NR protons normally found at $\delta = 0.42$ ppm for the free aminoalkene appears as a well-resolved triplet at lower field for **17** and **18** ($\delta = 0.72$ and 0.85 ppm). X-ray crystals of **17** suitable for diffraction studies were grown from a concentrated solution in pentane, and its solid-state structure was determined (Figure 13). To our knowledge, **17**

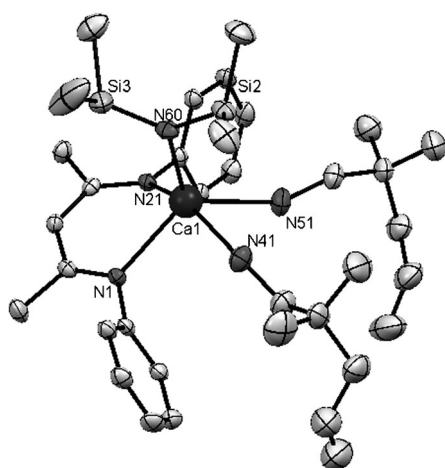


Figure 13. Solid-state structure of $[(\text{BDI})\text{AeN}(\text{SiMe}_2\text{H})_2][\text{H}_2\text{NCH}_2\text{C}(\text{CH}_3)_2\text{CH}_2\text{CH}=\text{CH}_2]$ (**17**). Only the main component of the aryl group is represented. The noninteracting solvent molecule, isopropyl groups, and hydrogen atoms are omitted for clarity. Ellipsoids are drawn at the 50% probability level. Selected bond lengths [\AA] and angles [$^\circ$]: Ca1–N60 2.333(2), Ca1–N21 2.394(2), Ca1–N1 2.403(2), Ca1–N41 2.545(2), Ca1–N51 2.560(2); N60–Ca1–N21 113.94(7), N60–Ca1–N1 116.94(7), N60–Ca1–N41 91.30(8), N60–Ca1–N51 119.86(8), Si2–N60–Ca1 114.6(1), Si3–N60–Ca1 118.9(1), Si2–N60–Si3 126.5(1).

represents the very first example of the structural characterization of a Ca–aminoalkene adduct. The Ca center is five-coordinate and sits in a geometry that averages as distorted-square-pyramidal and trigonal-bipyramidal environments ($\tau = 0.53$).^[43] The Si2–N60–Si3 angle of 126.5° resembles closely that found in **12**. The Ca–N bond lengths to the N atoms in the coordinated amine (2.54–2.56 \AA) are much longer than those to the N atoms from the β -diketiminate core (2.39–2.40 \AA), whereas the Ca–N60 bond length is even shorter (2.33 \AA). Unsurprisingly, the C=C double bonds of the aminoalkenes are not coordinated to the metal center.

Upon heating solutions of complexes **17** and **18** in $[\text{D}_6]$ benzene to 80°C , the gradual but quantitative formation of 2,4,4-trimethylpyrrolidine was observed by using ^1H NMR spectroscopy (Scheme 4; complexes **21** and **22**). Attempts to crystallize a metallic complex from these mixtures failed, but coordination of the cyclic amine moiety onto the metal center was established by means of NMR spectroscopy. Moreover, it proved impossible to remove the cyclic product by extraction with pentane and application of dynamic vacuum, even upon gentle heating. The relative ease of the cyclization of the aminoalkene in these complexes and their excellent solubility in aromatic solvents encouraged us to interrogate their reactivity, and our efforts focused on the more reactive **17**. The evolution of a solution of **17** in $[\text{D}_6]$ benzene was monitored by VT ^1H NMR spectroscopy at several temperatures in the range $50\text{--}80^\circ\text{C}$. We found that in all cases cyclization of the two equivalents of the aminoalkene versus Ca occurred without an induction period and with first-order dependence upon the concentration in **17**.^[26] The activation energy value of 103.1 kJ mol^{-1} was extracted from the Arrhenius plot (Figure 14); furthermore, the use of Eyring analysis disclosed a high activation enthalpy ($\Delta H^\ddagger = 102.4(6.7)\text{ kJ mol}^{-1}$) and a rather low acti-

vation entropy ($\Delta S^\ddagger = -21.9(3.2) \text{ J mol}^{-1} \text{ K}^{-1}$), with a corresponding activation Gibbs energy of $\Delta G^\ddagger = 108.9 \text{ kJ mol}^{-1}$ at 298 K.

The ^1H NMR spectroscopic monitoring at 80°C of the cyclization of the two molecules of **B** coordinated onto the metal center in **17** gave an initial $k_{\text{obs},17}^1$ value of $5.5 \times 10^{-4} \text{ s}^{-1}$ (Figure 15).^[44] There was no evidence for the presence of

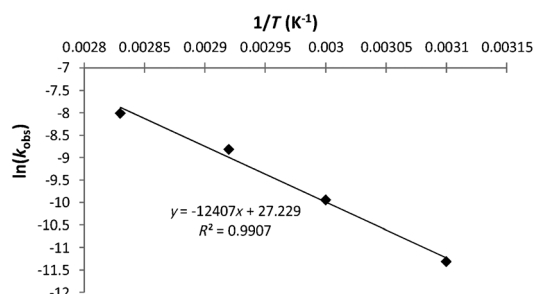


Figure 14. Arrhenius plot for the cyclization of the coordinated aminoalkene **B** in the complex $[(\text{BDI})\text{CaN}(\text{SiMe}_2\text{H})_2[\text{H}_2\text{NCH}_2\text{C}(\text{CH}_3)_2\text{CH}_2\text{CH}=\text{CH}_2]_2]$ (**17**) upon heating a solution of **17** (20 μmol) in $[\text{D}_6]$ benzene (0.4 mL).

uncoordinated **B** during this reaction; besides, the ^1H NMR data recorded after full conversion were consistent with coordination of both molecules of 2,4,4-trimethylpyrrolidine onto the Ca center (i.e., **21**). After complete conversion of the aminoalkene had been ensured, a second batch of **B** (2 equiv) was introduced into the reaction mixture, and the measured observed rate constant for this second batch of substrate was $k_{\text{obs},17}^2 = 5.7 \times 10^{-4} \text{ s}^{-1}$. A third batch of two equivalents of **B** was fully converted with $k_{\text{obs},17}^3 = 5.4 \times 10^{-4} \text{ s}^{-1}$. The near-identical values of k_{obs} determined during the conversion of three consecutive batches of two equivalents of **B** versus Ca confirmed the excellent reproducibility of the measurements and indicated that the catalytically active species associated to **17** did not suffer from product inhibition nor catalyst decay. In a similar set of experiments, the THF adduct **11** was employed to convert three succes-

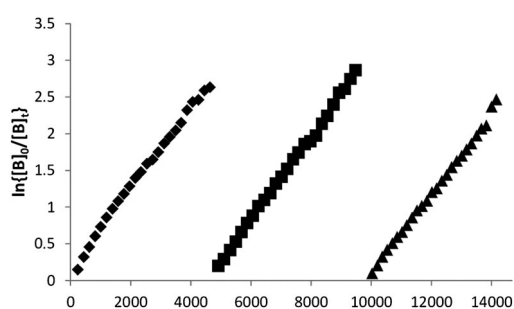


Figure 15. Sequential semilogarithmic plots for the conversion of the aminoalkene **B** in $[(\text{BDI})\text{CaN}(\text{SiMe}_2\text{H})_2[\text{H}_2\text{NCH}_2\text{C}(\text{CH}_3)_2\text{CH}_2\text{CH}=\text{CH}_2]_2]$ (**17**; $k_{\text{obs},17}^1 = 5.5 \times 10^{-4} \text{ s}^{-1}$; \blacklozenge), followed by conversion of two additional batches of two equivalents of **B** versus Ca ($k_{\text{obs},17}^2 = 5.7 \times 10^{-4} \text{ s}^{-1}$; \blacksquare and \blacktriangle) using 20 mmol of **17** in $[\text{D}_6]$ benzene (0.4 mL) at 80°C .

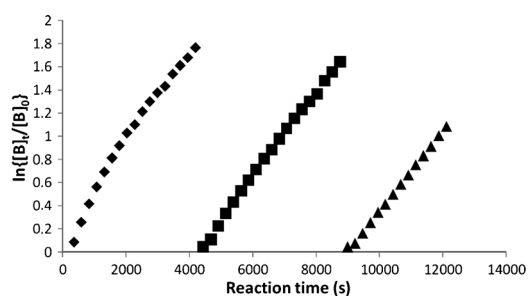


Figure 16. Sequential semilogarithmic plots for the conversion of the two equivalents of aminoalkene **B** in $[(\text{BDI})\text{CaN}(\text{SiMe}_2\text{H})_2(\text{thf})]$ (**11**; $k_{\text{obs},11}^1 = 4.2 \times 10^{-4} \text{ s}^{-1}$; \blacklozenge), followed by conversion of two additional batches of two equivalents of **B** versus Ca ($k_{\text{obs},11}^2 = 3.7 \times 10^{-4} \text{ s}^{-1}$; \blacksquare and \blacktriangle) using 20 mmol of **11** in $[\text{D}_6]$ benzene (0.4 mL) at 80°C .

sive batches of two equivalents of **B** (Figure 16), with the corresponding values $k_{\text{obs},11}^1 = 4.2 \times 10^{-4} \text{ s}^{-1}$, $k_{\text{obs},11}^2 = 3.7 \times 10^{-4} \text{ s}^{-1}$, and $k_{\text{obs},11}^3 = 3.4 \times 10^{-4} \text{ s}^{-1}$, respectively. Again, the values of k_{obs} were constant (within experimental error), and they were commensurate with those values determined for **17** and with the value determined during the cyclization of 12 equivalents of **B** versus **11** (Figure 5; $k_{\text{obs}} = 10.3 \times 10^{-4} \text{ s}^{-1}$).

Conclusion

The complexes of the large alkaline-earth metals $[(\text{LO}^i)\text{AeN}(\text{SiMe}_2\text{R})_2(\text{thf})_x]$ ($i = 1-4$; Ae = Ca, Sr, Ba; R = H, Me; $x = 0-2$) constitute the first examples of competent Ae-aminophenolate catalysts for the cyclohydroamination of two types of terminal aminoalkene. Cyclization occurred in all cases according to the guidelines developed by Baldwin, and the expected Thorpe–Ingold effect was observed. The complexes $[(\text{BDI})\text{AeN}(\text{SiMe}_2\text{H})_2(\text{thf})_x]$ (Ae = Ca, Sr, Ba, $x = 1-2$) and $[(\text{BDI})\text{CaN}(\text{SiMe}_3)_2(\text{thf})]$ supported by the ubiquitous β -diketiminato (BDI^-) ligand were also utilized. This last complex, reported by Hill and co-workers, displayed the greatest efficacy of all the tested catalysts by a long margin. General trends were established, which are given as follows:

1) For a given ligand, the catalytic activity decreases in the order $\text{Ca} > \text{Sr} \gg \text{Ba}$, that is, the smaller the metal center, the more effective the catalyst. This trend is the same as that observed and largely documented by Hill and co-workers for intramolecular cyclohydroamination reactions catalyzed by a variety of alkaline-earth complexes.^[9] Yet, it is the exact opposite of the trend previously observed during intermolecular hydroamination and hydrophosphination reactions of activated alkenes catalyzed by three complete families of charge-neutral heteroleptic alkaline-earth metal complexes.^[24] It is not clear at this stage why the activity trends are reversed on moving from inter- to intramolecular hydroamination reactions, and DFT calculations have so far not been conclusive. Hill and co-workers reported the inability of Ba complexes to catalyze the cyclohydroamination of **B** and argued that this behavior was probably a conse-

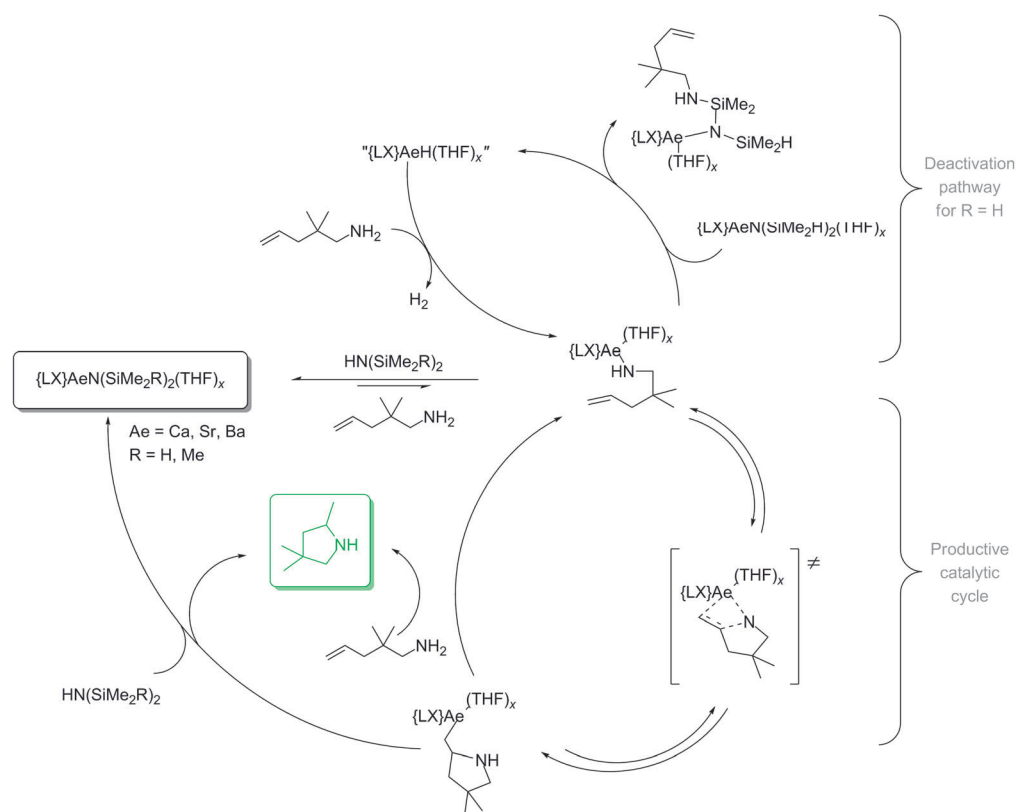
quence of the inability of the large Ba centers to sufficiently polarize the C=C double bond to enable its insertion into the Ba–N bond.^[9g] Yet, the excellent catalytic behavior of Ba complexes during intermolecular hydroamination reactions^[24] along with the moderate activity displayed by **3**, **(6)**₂ and **13** toward aminoalkenes **A** and **B** suggest this might be too simplistic an interpretation. By considering the large variation of the ionic radius between Ca, Sr, and Ba together with the different nature of intramolecular (cyclization of a single molecule) and intermolecular (coupling of two substrates) reactions, it may be pertinent to consider that entropic factors in fundamentally highly congested transition states are of utmost significance.

2) For a given metal center (Ca was used for convenience), catalyst performance increases when the chelating and donating ability of the aminophenolate ligand decreases. This finding can be interpreted both in terms of steric congestion, the availability of coordination sites on the central atom for the incoming substrate, and electronic considerations because the more electron-rich the metal center, the lower its ability to polarize the alkene and favor its insertion into the Ae–N bond.

3) For a given ligand framework and metal center, complexes that incorporate the N(SiMe₃)₂[–] amido group are catalytically far superior to their analogues that contain the N(SiMe₂H)₂[–] amide. This outcome is in striking contrast with other catalytic processes^[22k,n,23,24] and this observation could

find two explanations. First, the lower basicity of the N(SiMe₂H)₂[–] ion in comparison with the N(SiMe₃)₂[–] ion, thus resulting in a less favorable shift of the aminoalkene/amide exchange equilibrium [Eq. (2)]. Secondly, in the case of the [(LO⁺)AeN(SiMe₂H)₂(thf)_x] phenolate complexes, a case of catalyst deactivation through dehydrogenative coupling of the amine and hydrosilane was identified, thus readily leading, even at room temperature, to the formation of a catalytically inert alkaline-earth complex. This decomposition pathway was not necessarily specific to catalysts supported by aminophenolate ligands because similar N–Si dehydrogenative coupling was evidenced between [(BDI)AeN(SiMe₂H)₂(thf)_x] (Ae = Ca, Sr) and 2-methoxyethylamine, albeit under slightly more forcing conditions than those required for effective hydroamination catalysis. This finding led us to propose the extended mechanistic scenario depicted in Scheme 5 for cyclohydroamination catalyzed by [(LX)AeN(SiMe₂H)₂(thf)_x] complexes ((LX)[–] = (LO⁺)[–] or (BDI)[–]). We conclude that, although beneficial for the synthesis of stable alkaline-earth complexes owing to stabilization by internal Ae···H–Si agostic interactions, the use of the N(SiMe₂H)₂[–] ion may be prejudicial to catalytic activity in the case of catalyzed reactions involving reactive amine substrates (and possibly other Z–H active substrates).

Kinetic studies hinted at other subtleties. In the cases of catalysts bearing the ligands (BDI)[–] or (LO⁺)[–], first-order dependence upon initial substrate concentration was deter-



Scheme 5. Mechanisms for cyclohydroamination catalyzed by [(LX)AeN(SiMe₂H)₂(thf)_x].

mined. On the other hand, consumption of the substrate with $[(\text{LO}^1)\text{CaN}(\text{SiMe}_2\text{H})_2]$ and $[(\text{LO}^1)\text{CaN}(\text{SiMe}_3)_2]$ was independent from the substrate concentration; furthermore, the former complex exhibited inhibition by the substrate and product, whereas no evidence of these inhibitions were detected for the latter. These cases are further illustrations of the fine interplay between catalytic activity (and operative mechanisms) and the nature of the metal center, ligand scaffold, and amido groups. It is apparent from these results that the excessively simplistic mechanism given in Scheme 5 cannot be generalized for all alkaline-earth metal hydroamination catalysts and that further studies are required. The isolation of $[(\text{BDI})\text{CaN}(\text{SiMe}_2\text{H})_2]\{\text{H}_2\text{NCH}_2\text{C}(\text{CH}_3)_2\text{CH}_2\text{CH}=\text{CH}_2\}$ (**17**), the first example of a Ca–aminoalkene adduct structurally characterized, is a first step in this direction. This unique complex essentially behaves like the more standard $[(\text{BDI})\text{CaN}(\text{SiMe}_2\text{H})(\text{thf})]$ complex (**11**). NMR spectroscopic monitoring experiments indicate that both aminoalkene molecules remain coordinated to the Ca center under catalytic conditions and that after complete cyclization the final product is also tightly bound to the metal center. We are now investigating the use of this and related alkaline-earth complexes for the cyclohydroamination of a broad range of substrates.

Experimental Section

General procedures: All manipulations were performed in an inert atmosphere by using standard Schlenk techniques or in a Jacomex glove box ($\text{O}_2 < 1$ ppm, $\text{H}_2\text{O} < 5$ ppm) for catalyst loading. NMR spectra were recorded on Bruker AC-300, AC-400, and AM-500 spectrometers. ^1H and ^{13}C chemical shifts were determined by using the residual signals of the deuterated solvents and were calibrated versus SiMe_4 . Assignment of the signals was carried out using 1D (^1H , $^{13}\text{C}\{^1\text{H}\}$) and 2D (COSY, HMBC, HMQC) NMR experiments. $^{19}\text{F}\{^1\text{H}\}$ chemical shifts were determined by an external reference to an aqueous solution of NaBF_4 . ^{29}Si chemical shifts are reported relative to SiMe_4 . Elemental analyses were performed on a Carlo Erba 1108 Elemental Analyzer instrument at the London Metropolitan University by Stephen Boyer and were the average of a minimum of two independent measurements. FTIR spectra were recorded at room temperature as nujol mulls in KBr plates on a Shimadzu Affinity-IR spectrometer. CaI_2 , SrI_2 , and BaI_2 (anhydrous beads; 99.995%) were purchased from Aldrich and used as received. Reagents $\text{HN}(\text{SiMe}_3)_2$ (Acros), $\text{HN}(\text{SiMe}_2\text{H})_2$ (ABCR), and 2-methoxyethylamine (Acros) were dried over activated 3 Å molecular sieves and distilled under reduced pressure prior to use. The substrates 1-amino-2,2-diphenyl-4-pentene (**A**) and 1-amino-2,2-dimethyl-4-pentene (**B**) were synthesized according to a reported procedure.^[45] Toluene was distilled under argon from melted sodium prior to use. THF was first predried over sodium hydroxide and distilled under argon over CaH_2 , and then freshly distilled a second time under argon from Na/benzophenone prior to use. Et_2O , dichloromethane, and pentane were distilled under argon from Na/benzophenone, CaH_2 , and Na/benzophenone/tetraglyme, respectively. All the deuterated solvents (Eurisotop, Saclay, France) were stored in sealed ampoules over activated 3 Å molecular sieves and were degassed by several freeze–thaw cycles. The precursors $[\text{Ae}\{\text{N}(\text{SiMe}_3)_2\}_2(\text{thf})_2]$ ($\text{Ae} = \text{Ca}$, Sr , Ba)^[22e, 46] and $[\text{Ae}\{\text{N}(\text{SiMe}_2\text{H})_2\}_2(\text{thf})_2]$ ($\text{Ae} = \text{Ca}$, $x = 1$; Sr , $x = 2/3$; Ba , $x = 0$)^[22k] the complexes $[(\text{LO}^x)\text{CaN}(\text{SiMe}_3)_2]$ (**1**)^[22l] $[(\text{LO}^x)\text{SrN}(\text{SiMe}_3)_2(\text{thf})]$ (**2**)^[24] $[(\text{LO}^x)\text{BaN}(\text{SiMe}_3)_2(\text{thf})]$ (**3**)^[22ml] $[(\text{LO}^x)\text{CaN}(\text{SiMe}_2\text{H})_2(\text{thf})]$ (**4**)^[22nl] $[(\text{LO}^x)\text{BaN}(\text{SiMe}_2\text{H})_2(\text{thf})]$ (**6**)^[22nl] $[(\text{LO}^1)\text{CaN}(\text{SiMe}_2\text{H})_2]$ (**7**)^[22nl] $[(\text{LO}^2)\text{CaN}(\text{SiMe}_2\text{H})_2]$ (**8**)^[22nl] $[(\text{LO}^3)\text{CaN}(\text{SiMe}_2\text{H})_2]$ (**9**)^[22nl] $[(\text{LO}^1)\text{CaN}(\text{SiMe}_3)_2]$ (**10**)^[22nl] and $[(\text{BDI})\text{AeN}(\text{SiMe}_2\text{H})_2(\text{thf})_x]$ ($\text{Ae} = \text{Ca}$, $x = 1$) (**11**);

Sr , $x = 2$ (**12**); Ba , $x = 2$ (**13**)^[24] and the proligands $(\text{LO})^i\text{H}$ ($i = 1-4$)^[47] and $(\text{BDI})\text{H}$ ^[48] were all prepared as described elsewhere.

$[(\text{LO}^4)\text{SrN}(\text{SiMe}_2\text{H})_2]$ (5**)₂:** A mixture of $[\text{Sr}\{\text{N}(\text{SiMe}_3)_2\}_2(\text{thf})_2]$ (0.43 g, 0.78 mmol) and $\text{HN}(\text{SiMe}_2\text{H})_2$ (0.27 mL, 0.78 mmol) was stirred in Et_2O (10 mL) overnight at room temperature. After addition of a solution of $(\text{LO}^4)\text{H}$ (0.26 g, 0.74 mmol) in Et_2O (5 mL), a white precipitate formed slowly upon stirring at room temperature. The suspension was stirred for a further 6 h, and the precipitate was isolated by filtration. Following drying to constant weight, (**5**)₂ was obtained as a colorless powder (0.31 g, 73%). Recrystallization from a concentrated solution of (**5**)₂ in benzene afforded X-ray quality single crystals. The dimeric complex showed very poor solubility in aromatic solvents and highly dynamic behavior in $[\text{D}_8]\text{THF}$, which is indicative of significant dissociation in this solvent (assignments for both the monomeric and dimeric complexes are given).

For the monomer: ^1H NMR ($[\text{D}_8]\text{THF}$, 298 K, 400.1 MHz): $\delta = 7.32$ (d, $^4J_{\text{HH}} = 2.6$ Hz, 1H; *m*-H), 6.99 (d, $^4J_{\text{HH}} = 2.6$ Hz, 1H; *m*-H), 4.98 (m, $^1J_{\text{SiH}} = 164$ Hz, 2H; *SiH*), 3.94 (br, 2H; ArCH_2N), 3.84 (brs, 4H; CH_2O), 3.76 (s, 6H; OCH_3), 2.91 (d, $^4J_{\text{HH}} = 2.6$ Hz, 4H; NCH_2CH_2), 1.68 (s, 9H; *o*- $\text{C}(\text{CH}_3)_3$), 1.48 (s, 9H; *p*- $\text{C}(\text{CH}_3)_3$), 0.29 ppm (d, $^3J_{\text{HH}} = 2.3$ Hz, 12H; $\text{Si}(\text{CH}_3)_2\text{H}$); ^{13}C NMR ($[\text{D}_8]\text{THF}$, 298 K, 100.6 MHz): $\delta = 166.7$ (*i*-C), 136.4 (*o*-C), 131.4 (*p*-C), 126.7 (*o*-C), 123.8 (*m*-C), 123.4 (*m*-C), 71.2 (CH_2O), 62.2 (ArCH_2N), 60.5 (OCH_3), 54.4 (NCH_2CH_2), 36.1 (*o*- $\text{C}(\text{CH}_3)_3$), 34.4 (*p*- $\text{C}(\text{CH}_3)_3$), 32.8 (*p*- $\text{C}(\text{CH}_3)_3$), 30.7 (*o*- $\text{C}(\text{CH}_3)_3$), 5.3 ppm ($\text{Si}(\text{CH}_3)_2\text{H}$); ^{29}Si NMR ($[\text{D}_8]\text{THF}$, 298 K, 79.5 MHz): $\delta = -26.85$ ppm.

For the dimer: ^1H NMR ($[\text{D}_8]\text{THF}$, 298 K, 400.1 MHz): $\delta = 7.28$ (d, $^4J_{\text{HH}} = 2.6$ Hz, 2H; *m*-H), 6.94 (d, $^4J_{\text{HH}} = 2.6$ Hz, 2H; *m*-H), 4.91 (m, $^1J_{\text{SiH}} = 162$ Hz, 4H; *SiH*), 3.90 (br, 4H; ArCH_2N), 3.82 (br s, 8H; CH_2O), 3.72 (s, 12H; OCH_3), 1.99 (br s, 8H; NCH_2CH_2), 1.68 (s, 18H; *o*- $\text{C}(\text{CH}_3)_3$), 1.48 (s, 18H; *p*- $\text{C}(\text{CH}_3)_3$), 0.26 ppm (d, $^3J_{\text{HH}} = 2.8$ Hz, 24H; $\text{Si}(\text{CH}_3)_2\text{H}$); ^{13}C NMR ($[\text{D}_8]\text{THF}$, 298 K, 100.6 MHz): $\delta = 167.9$ (*i*-C), 135.8 (*o*-C), 129.7 (*p*-C), 126.8 (*o*-C), 123.4 (*m*-C), 122.7 (*m*-C), 69.9 (CH_2O), 60.4 (OCH_3), 60.1 (ArCH_2N), 53.4 (NCH_2CH_2), 36.0 (*o*- $\text{C}(\text{CH}_3)_3$), 34.4 (*p*- $\text{C}(\text{CH}_3)_3$), 32.8 (*p*- $\text{C}(\text{CH}_3)_3$), 30.6 (*o*- $\text{C}(\text{CH}_3)_3$), 5.2 ppm ($\text{Si}(\text{CH}_3)_2\text{H}$); ^{29}Si NMR ($[\text{D}_8]\text{THF}$, 298 K, 79.5 MHz): $\delta = -26.90$ ppm; FTIR (nujol in KBr plates): $\tilde{\nu} = 2005$ (s), 1971 (s), 1917 (s), 1771 (w), 1602 cm^{-1} (s); elemental analysis (%) calcd for $\text{C}_{50}\text{H}_{100}\text{N}_4\text{O}_4\text{Si}_4\text{Sr}_2$ (1140.92 g mol^{-1}): C 52.64, H 8.83, N 4.91; found: C 52.46, H 8.75, N 4.79.

$[(\text{LO}^4)\text{CaN}(\text{SiMe}_2\text{H})(\text{SiMe}_2\text{NHCH}_2\text{CH}_2\text{OCH}_3)]$ (14**):** 2-Methoxyethylamine (32 μL , 0.37 mmol) was added slowly to a solution of **4** (200 mg, 0.34 mmol) in toluene (3 mL) at room temperature. After 3 h, the reaction solution was concentrated to 0.5 mL and diluted by the addition of pentane (1.5 mL). Fractionated crystallization at -30°C over the course of several days afforded **14** as colorless crystals (60 mg, 31%) suitable for X-ray diffraction studies. ^1H NMR ($[\text{D}_6]\text{benzene}$, 298 K, 400.1 MHz): $\delta = 7.57$ (d, $^4J_{\text{HH}} = 2.8$ Hz, 1H; *m*-H), 7.02 (d, $^4J_{\text{HH}} = 2.8$ Hz, 1H; *m*-H), 5.09 (m, $^1J_{\text{SiH}} = 172$ Hz, 1H; SiMe_2H), 3.35 (t, $^3J_{\text{HH}} = 4.8$ Hz, 2H; $\text{CH}_2\text{CH}_2\text{NH}$), 3.28 (br s, 2H; ArCH_2N), 3.13 (s, 6H; $\text{CH}_2\text{NCH}_2\text{CH}_2\text{OCH}_3$), 3.07 (s, 3H; $\text{CH}_3\text{OCH}_2\text{CH}_2\text{NH}$), 2.97 (m, 4H; $\text{CH}_2\text{NCH}_2\text{CH}_2$), 2.76 (m, 2H; $\text{CH}_2\text{CH}_2\text{NH}$), 2.18 (m, 4H; $\text{CH}_2\text{NCH}_2\text{CH}_2$), 1.78 (s, 9H; *o*- $\text{C}(\text{CH}_3)_3$), 1.51 (s, 9H; *p*- $\text{C}(\text{CH}_3)_3$), 0.92 (t, $^3J_{\text{HH}} = 7.8$ Hz, 1H; $\text{CH}_2\text{CH}_2\text{NH}$), 0.38 (d, $^3J_{\text{HH}} = 2.8$ Hz, 6H; $\text{NSi}(\text{CH}_3)_2\text{H}$), 0.33 ppm (s, 6H; $\text{NSi}(\text{CH}_3)_2\text{NH}$); ^{13}C NMR ($[\text{D}_6]\text{benzene}$, 298 K, 100.6 MHz): $\delta = 165.9$ (*i*-C), 135.3 (*o*-C), 131.3 (*p*-C), 125.5 (*o*-C), 123.4 (*m*-C), 122.9 (*m*-C), 74.9 ($\text{CH}_2\text{CH}_2\text{NH}$), 69.4 ($\text{CH}_2\text{NCH}_2\text{CH}_2\text{O}$), 62.5 (ArCH_2N), 59.4 ($\text{CH}_3\text{OCH}_2\text{CH}_2\text{NCH}_2$), 58.6 ($\text{CH}_3\text{OCH}_2\text{CH}_2\text{NH}$), 54.3 ($\text{CH}_2\text{NCH}_2\text{CH}_2\text{O}$), 41.7 ($\text{CH}_2\text{CH}_2\text{NH}$), 35.3 (*o*- $\text{C}(\text{CH}_3)_3$), 33.7 (*p*- $\text{C}(\text{CH}_3)_3$), 32.2 (*p*- $\text{C}(\text{CH}_3)_3$), 29.9 (*o*- $\text{C}(\text{CH}_3)_3$), 4.75 ($\text{Si}(\text{CH}_3)_2\text{H}$), 3.67 ppm ($\text{Si}(\text{CH}_3)_2\text{NH}$); ^{29}Si NMR ($[\text{D}_6]\text{benzene}$, 298 K, 79.5 MHz): $\delta = -13.25$ ($\text{Si}(\text{CH}_3)_2\text{NH}$), -30.06 ppm ($\text{Si}(\text{CH}_3)_2\text{H}$); elemental analysis (%) calcd for $\text{C}_{28}\text{H}_{57}\text{CaN}_3\text{Si}_2\text{O}_4$ (596.02 g mol^{-1}): C 56.42, H 9.64, N 7.05; found: C 56.50, H 9.58, N 6.98.

$[(\text{BDI})\text{CaN}(\text{SiMe}_2\text{H})_2(\text{NH}_2\text{CH}_2\text{CH}_2\text{OCH}_3)]$ (15**):** 2-Methoxyethylamine (31 μL , 0.35 mmol) was added slowly to a solution of **11** (210 mg, 0.32 mmol) in pentane (3 mL) at room temperature. A white precipitate gradually appeared. After 3 h, this solid was isolated by cannula filtration and dried under vacuum. The solution was kept at -30°C to afford two

crops of **15** as colorless crystals after crystallization (180 mg, 85%). ¹H NMR ([D₆]benzene, 298 K, 400.1 MHz): δ = 7.09 (m, 6H; arom-*H*), 4.93 (s, 1H; MeCCHCMe), 4.89 (m, ¹J_{SiH} = 159 Hz, 2H; SiH), 3.62 (m, 2H; CH(CH₃)₂), 3.31 (m, 2H; CH(CH₃)₂), 2.47 (t, ³J_{HH} = 4.5 Hz, 2H; MeOCH₂), 2.19 (s, 3H; CH₃O), 1.80 (br, 2H; CH₂NH₂), 1.72 (s, 6H; (CH₃)CCHC(CH₃)), 1.46–1.15 (m, 24H; CH(CH₃)₂), 0.48 (d, ³J_{HH} = 2.9 Hz, 12H; SiMe₂H), 0.31 ppm (brm, 2H; CH₂NH₂); [¹H]¹³C NMR ([D₆]benzene, 298 K, 100.6 MHz): δ = 166.0 (C(Me)=N), 149.7 (*i*-C), 143.3 (*o*-C), 124.5 (*p*-C), 124.1 (*m*-C), 95.9 (MeCCHCMe), 73.1 (MeOCH₂), 59.0 (CH₃O), 40.8 (CH₂NH₂), 29.1 (CH(CH₃)₂), 25.6 (CH(CH₃)₂), 25.3 ((CH₃)CCHC(CH₃)), 5.2 ppm (Si(CH₃)₂H); [¹H]²⁹Si NMR ([D₆]benzene, 298 K, 79.5 MHz): δ = -25.52 ppm; satisfactory elemental analysis for this compound could not be obtained reliably.

[(BDI)SrN(SiMe₂H)₂(NH₂CH₂CH₂OCH₃)] (16): Following an identical protocol to that described for **15**, the reaction of 2-methoxyethylamine (31 μL, 0.35 mmol) and **12** (250 mg, 0.32 mmol) afforded **16** as colorless crystals (200 mg, 88%). ¹H NMR ([D₆]benzene, 298 K, 500.1 MHz): δ = 7.11 (d, ³J_{HH} = 7.2 Hz, 4H; *m*-H), 7.04 (t, ³J_{HH} = 7.2 Hz, 2H; *p*-H), 4.92 (m, ¹J_{SiH} = 184 Hz, 2H; SiH), 4.89 (s, 1H; MeCCHCMe), 3.43 (m, 4H; CH(CH₃)₂), 2.37 (t, ³J_{HH} = 4.5 Hz, 2H; OCH₂), 2.14 (s, 3H; CH₃O), 1.75 (brm, 8H; (CH₃)CCHC(CH₃) + CH₂NH₂), 1.30 (d, ³J_{HH} = 7.0 Hz, 24H; CH(CH₃)₂), 0.47 (d, ³J_{HH} = 3.0 Hz, 12H; Si(CH₃)₂H), -0.04 ppm (brm, 2H; CH₂NH₂); [¹H]¹³C NMR ([D₆]benzene, 298 K, 125.8 MHz): δ = 164.9 (C(Me)=N), 149.2 (*i*-C), 142.6 (*o*-C), 124.3 (*p*-C), 124.1 (*m*-C), 94.9 (MeCCHCMe), 73.5 (MeOCH₂), 58.6 (CH₃O), 41.4 (CH₂NH₂), 28.6 (CH(CH₃)₂), 25.3 (CH(CH₃)₂), 25.3 ((CH₃)CCHC(CH₃)), 5.2 ppm (Si(CH₃)₂H); [¹H]²⁹Si NMR ([D₆]benzene, 298 K, 79.5 MHz): δ = -27.57 ppm; FTIR (nujol in KBr plates): $\tilde{\nu}$ = 1992 (sh), 1986 (s), 1925 (m), 1550 cm⁻¹ (s); elemental analysis (%) calcd for C₃₀H₆₄SrN₄O₅Si₂ (712.71 g mol⁻¹): C 60.67, H 9.05, N 7.86; found: C 60.58, H 9.09, N 7.73.

[(BDI)CaN(SiMe₂H)₂(NH₂CH₂C(Me)CH₂CH=CH₂)] (17): 1-Amino-2,2-dimethyl-4-pentene (70 mg, 0.62 mmol) was added slowly to a solution of **11** (0.19 g, 0.28 mmol) in pentane (5 mL) at room temperature. After 3 h, removal of the solvent under vacuum yielded a light yellow solid, which was purified by washing with pentane (4 mL) and dried in vacuo. This procedure was repeated three times to give **17** quantitatively after drying to a constant weight (220 mg, 95%). X-ray quality crystals were grown from a solution of **17** in pentane stored at -30 °C with very slow evaporation of the solvent. ¹H NMR ([D₆]benzene, 298 K, 500.1 MHz): δ = 7.09 (d, ³J_{HH} = 7.2 Hz, 4H; *m*-H), 7.02 (t, ³J_{HH} = 7.2 Hz, 2H; *p*-H), 5.61 (m, 2H; CH₂=CHCH₂), 5.02–4.99 (m, 4H; CH₂=CHCH₂), 4.96 (m, 2H; SiH), 4.88 (s, 1H; MeCCHCMe), 3.46 (m, 4H; CH(CH₃)₂), 2.07 (t, ³J_{HH} = 3.6 Hz, 4H; CH₂NH₂), 1.72 (s, 6H; (CH₃)CCHC(CH₃)), 1.67 (d, ³J_{HH} = 3.6 Hz, 4H; CH₂=CHCH₂), 1.36 (d, ³J_{HH} = 7.0 Hz, 12H; CH(CH₃)₂), 1.28 (d, ³J_{HH} = 7.0 Hz, 12H; CH(CH₃)₂), 0.72 (t, ³J_{HH} = 8.5 Hz, 4H; CH₂NH₂), 0.56 (s, 12H; CH₂C(CH₃)₂CH₂), 0.43 ppm (d, ³J_{HH} = 3.0 Hz, 12H; Si(CH₃)₂H); [¹H]¹³C NMR ([D₆]benzene, 298 K, 125.8 MHz): δ = 166.4 (C(Me)=N), 149.4 (*i*-C), 142.4 (*o*-C), 135.0 (CH₂=CCHCH₂), 124.8 (*p*-C), 124.1 (*m*-C), 118.3 (CH₂=CHCH₂), 95.2 (MeCCHCMe), 53.5 (CH₂NH₂), 44.9 (CH₂=CHCH₂), 35.3 (C(CH₃)₂), 28.6 (CH(CH₃)₂), 26.0 (C(CH₃)₂), 25.7 (CH(CH₃)₂), 25.3 (CH(CH₃)₂), 25.0 ((CH₃)CCHC(CH₃)), 5.4 ppm (Si(CH₃)₂H); [¹H]²⁹Si NMR ([D₆]benzene, 298 K, 79.5 MHz): δ = -24.64 ppm; FTIR (nujol in KBr plates): $\tilde{\nu}$ = 2025 (s), 1924 (w), 1624 (w), 1581 (m), 1539 (s), 1516 cm⁻¹ (s); elemental analysis (%) calcd for C₄₇H₈₅CaN₅Si₂ (816.46 g mol⁻¹): C 69.14, H 10.49, N 8.58; found: C 69.04, H 10.53, N 8.62.

[(BDI)SrN(SiMe₂H)₂(NH₂CH₂C(Me)CH₂CH=CH₂)] (18): Following an identical procedure to that described for **17**, the reaction of 1-amino-2,2-dimethyl-4-pentene (90 mg, 0.79 mmol) and **12** (280 mg, 0.35 mmol) afforded **18** as a pale yellow powder (290 mg, 96%). ¹H NMR ([D₆]benzene, 298 K, 500.1 MHz): δ = 7.12 (d, ³J_{HH} = 7.2 Hz, 4H; *m*-H), 7.05 (t, ³J_{HH} = 7.2 Hz, 2H; *p*-H), 5.61 (m, 2H; CH₂=CHCH₂), 5.01–4.96 (m, 4H; CH₂=CHCH₂), 4.94 (m, 2H; SiH), 4.90 (s, 1H; MeCCHCMe), 3.44 (m, 4H; CH(CH₃)₂), 2.07 (t, ³J_{HH} = 3.6 Hz, 4H; CH₂NH₂), 1.69 (s, 6H; (CH₃)CCHC(CH₃)), 1.64 (d, ³J_{HH} = 3.6 Hz, 4H; CH₂=CHCH₂), 1.36 (d, ³J_{HH} = 7.0 Hz, 12H; CH(CH₃)₂), 1.26 (d, ³J_{HH} = 7.0 Hz, 12H; CH(CH₃)₂), 0.85 (t, ³J_{HH} = 8.5 Hz, 4H; CH₂NH₂), 0.54 (s, 12H; CH₂C(CH₃)₂CH₂), 0.40 ppm (d, ³J_{HH} = 3.0 Hz, 12H; Si(CH₃)₂H); [¹H]¹³C NMR

([D₆]benzene, 298 K, 125.8 MHz): δ = 165.1 (C(Me)=N), 149.7 (*i*-C), 142.3 (*o*-C), 135.1 (CH₂=CHCH₂), 124.7 (*p*-C), 124.1 (*m*-C), 118.3 (CH₂=CHCH₂), 94.9 (MeCCHCMe), 53.3 (CH₂NH₂), 44.7 (CH₂=CHCH₂), 35.4 (C(CH₃)₂), 28.5 (CH(CH₃)₂), 26.3 (C(CH₃)₂), 25.5 (CH(CH₃)₂), 25.2 (CH(CH₃)₂), 24.6 ((CH₃)CCHC(CH₃)), 5.2 ppm (Si(CH₃)₂H); [¹H]²⁹Si NMR ([D₆]benzene, 298 K, 79.5 MHz): δ = -26.85 ppm; FTIR (nujol in KBr plates): $\tilde{\nu}$ = 2017 (s), 1924 (w), 1960 (sh), 1624 (w), 1585 (m), 1543 (s), 1512 (s) cm⁻¹; elemental analysis (%) calcd for C₄₇H₈₅SrN₅Si₂ (864.00 g mol⁻¹): C 65.34, H 9.92, N 8.11; found: C 64.92, H 9.87, N 8.72.

¹H NMR data for [(BDI)CaN(SiMe₂H)₂(2,4,4-trimethylpyrrolidine)₂] (21) generated in situ: ([D₆]benzene, 353 K, 500.13 MHz): δ = 7.13 (dd, ³J_{HH} = 7.5, ⁴J_{HH} = 1.3 Hz, 4H; *m*-H), 7.07 (t, ³J_{HH} = 7.6 Hz, 2H; *p*-H), 4.90 (m, 2H; SiH; 1H; MeCCHCMe), 3.31 (hept, ³J_{HH} = 6.8 Hz, 4H; CH(CH₃)₂), 3.09 (m, 2H; NHCH(CH₃)CH₂H_b), 2.50 (dd, ²J_{HH} = 10.8, ³J_{HH} = 6.5 Hz, 2H; NHCH₂H_bC(CH₃)₂), 2.32 (dd, ²J_{HH} = 10.8, ³J_{HH} = 6.5 Hz, 2H; NHCH₂H_bC(CH₃)₂), 1.74 (s, 6H; (CH₃)CCHC(CH₃)), 1.50 (br, 2H; NHCH(CH₃)CH₂H_b), 1.44 (dd, ²J_{HH} = 12.5, ³J_{HH} = 7.2 Hz, 2H; NHCH(CH₃)CH₂H_b), 1.36 (d, ³J_{HH} = 6.8 Hz, 12H; CH(CH₃)₂), 1.27 (d, ³J_{HH} = 6.8 Hz, 12H; CH(CH₃)₂), 0.88–0.86 (overlap of: d, ³J_{HH} = 6.3 Hz, 6H and m, 2H for NHCH(CH₃)CH₂H_b and NHCH(CH₃)CH₂H_b, respectively), 0.84 (s, 6H; NHCH₂H_bC(CH₃)₂), 0.80 (s, 6H; NHCH₂H_bC(CH₃)₂), 0.29 ppm (d, ³J_{HH} = 2.9 Hz, 12H; Si(CH₃)₂H).

X-ray diffraction crystallography: Suitable crystals for X-ray diffraction analysis of (**5**), **12**, **14**, **16**, and **17** were obtained by recrystallization of the purified products. Diffraction data were collected at 150 K using a Bruker APEX CCD diffractometer with graphite-monochromated MoK α radiation (λ = 0.71073 Å). A combination of ω and ϕ scans was carried out to obtain at least a unique data set. The crystal structures were solved by direct methods, the remaining atoms were located from difference Fourier synthesis followed by full-matrix least-squares refinement based on *F*² (programs SIR97 and SHELXL-97).^[49] Many hydrogen atoms could be found from the Fourier-difference analysis. Carbon- and oxygen-bound hydrogen atoms were placed at calculated positions and forced to ride on the attached atom. The hydrogen-atom contributions were calculated but not refined. All non-hydrogen atoms were refined with anisotropic displacement parameters. The locations of the largest peaks in the final-difference Fourier-map calculation and the magnitude of the residual electron densities were of no chemical significance. The relevant collection and refinement data are summarized in Table 3. CCDC-900840 (**5**), CCDC-900841 (**12**), CCDC-900842 (**14**), CCDC-900843 (**16**), and CCDC-900844 (**17**) contain the supplementary crystallographic data for this paper. These data can be obtained free of charge from The Cambridge Crystallographic Data Centre via www.ccdc.cam.ac.uk/data_request/cif.

Protocol for NMR-scale cyclohydroamination reactions: Catalyzed cyclohydroamination reactions monitored by means of ¹H NMR spectroscopy were carried out by using the following procedure: In a glove-box, the catalyst was loaded into an NMR tube. By using Schlenk techniques, the substrate and [D₆]benzene (0.4 mL) were added into the NMR tube. The tube was sealed, vigorously shaken, and immersed into an oil bath preset at the desired temperature. After the required amount of time, the NMR tube was removed from the oil bath and the ¹H NMR spectrum of the reaction mixture was recorded. The conversion was calculated by comparing the relative intensities of resonance signals characteristic of the substrate and product.

NMR spectroscopic monitoring of cyclohydroamination reactions: Catalyzed cyclohydroamination reactions monitored by ¹H NMR spectroscopy were carried out by using the following procedure: In a glove-box, the catalyst was loaded into an NMR tube. By using Schlenk techniques, the substrate and [D₆]benzene (0.4 mL) were added into the NMR tube. The tube was sealed, vigorously shaken, and inserted into the probe of a Bruker AM 500 NMR spectrometer preheated to the required temperature. The reaction kinetics were monitored (using the multi_zgvd command; D1 = 0.2 s; DS = 0; NS = 8, or more) over the course of three or more half-lives on the basis of amine consumption by comparing the relative intensities of resonance signals characteristic of the substrate and product.

Table 3. Summary of crystallographic data for compounds (**5**)₂, **12**, **14**, **16**, and **17**.

	(5) ₂	12	14	16	17
empirical formula	C ₃₀ H ₁₀₀ N ₄ O ₆ Si ₄ Sr ₂	C ₄₁ H ₇₁ N ₅ O ₂ Si ₂ Sr	C ₂₈ H ₃₇ CaN ₃ O ₄ Si ₂	C ₃₆ H ₆₄ N ₄ O ₂ Si ₂ Sr	C ₄₇ H ₈₈ CaN ₅ Si ₂
CCDC number	900844	900840	900841	900842	900843
formula weight	1140.94	787.81	596.03	712.71	816.46
crystal system	triclinic	triclinic	monoclinic	monoclinic	monoclinic
space group	<i>P</i> $\bar{1}$	<i>P</i> $\bar{1}$	<i>P</i> ₂ / <i>1</i> / <i>n</i>	<i>Cc</i>	<i>P</i> ₂ / <i>1</i> / <i>n</i>
<i>a</i> [Å]	11.1741(2)	10.9482(9)	9.4997(4)	12.6035(9)	11.7644(5)
<i>b</i> [Å]	12.4674(3)	11.6660(9)	26.2765(11)	19.5047(13)	22.7348(10)
<i>c</i> [Å]	12.4791(3)	20.2339(18)	14.0987(5)	17.6446(12)	19.1741(8)
α [°]	63.1060(10)	85.017(3)	90	90	90
β [°]	88.9700(10)	11.6660(9)	96.991(2)	108.845(3)	91.284(2)
γ [°]	80.7940(10)	67.047(3)	90	90	90
volume [Å ³]	1527.57(6)	2360.6(3)	3493.1(2)	4105.0(5)	5127.0(4)
<i>Z</i>	2	2	4	4	4
ρ [g cm ⁻³]	1.240	1.100	1.133	1.153	1.058
μ [mm ⁻¹]	1.869	1.225	0.281	1.402	0.203
<i>F</i> (000)	608	840	1304	1528	1800
crystal size [mm]	0.40 × 0.28 × 0.20	0.57 × 0.46 × 0.23	0.54 × 0.16 × 0.09	0.54 × 0.37 × 0.23	0.55 × 0.53 × 0.18
θ range [°]	1.83–27.45	2.35–27.08	2.91–27.47	3.42–27.47	1.39–27.50
limiting indices	–14 < <i>h</i> < 12 –16 < <i>k</i> < 11 –16 < <i>l</i> < 16	–14 < <i>h</i> < 14 –11 < <i>k</i> < 15 –26 < <i>l</i> < 26	–10 < <i>h</i> < 10 –32 < <i>k</i> < 34 –18 < <i>l</i> < 18	–16 < <i>h</i> < 16 –25 < <i>k</i> < 25 –22 < <i>l</i> < 22	–15 < <i>h</i> < 15 –29 < <i>k</i> < 29 –20 < <i>l</i> < 24
<i>R</i> _{int}	0.0339	0.0384	0.0524	0.0327	0.0731
refl. collected	24433	27002	28920	30427	45915
refl. unique [<i>I</i> > 2 σ (<i>I</i>)]	6937	10581	7957	8867	68699
data/restraints/parameters	6937/0/325	10581/0/462	7957/0/362	8867/2/402	11681/0/522
goodness-of-fit on <i>F</i> ²	1.174	1.034	0.954	1.036	1.063
<i>R</i> ₁ [<i>I</i> > 2 σ (<i>I</i>)] (all data)	0.0377(0.1006)	0.0426 (0.0634)	0.0499 (0.1227)	0.0293 (0.0700)	0.0564 (0.1508)
<i>wR</i> ₂ [<i>I</i> > 2 σ (<i>I</i>)] (all data)	0.0502(0.1201)	0.1059 (0.1128)	0.0755 (0.1372)	0.0340 (0.0714)	0.0952 (0.1798)
largest difference [e Å ⁻³]	1.693 and –0.813	0.763 and –0.391	0.368 and –0.395	0.483 and –0.415	0.737 and –0.406

Details of the kinetic measurements with corresponding plots; Van't Hoff analysis and the FTIR spectrum of (**5**)₂; ¹H NMR spectroscopic monitoring of the reaction of **1** and 1-amino-2,2-dimethyl-4-pentene (**B**) in [D₆]benzene; crystallographic data of (**5**)₂, **12**, **14**, **16**, and **17** (as CIF files); and representation of the solid-state structure of **16** are given in the Supporting Information

Acknowledgements

Financial support from the European Research Council (Marie Curie FP7-PEOPLE-2010-IIF fellowship to B.L. ChemCatSusDe), the CNRS (Y.S.), and the Institut Universitaire de France (J.F.C.) is gratefully acknowledged. We thank Stephen Boyer (London Metropolitan University) for his assistance with elemental analyses.

- [1] *Catalytic Heterofunctionalization: from Hydroamination to Hydrozirconation* (Eds.: A. Togni, H. Grützmacher), Wiley-VCH, Weinheim, **2001**.
- [2] For reviews, see: a) T. E. Müller, M. Beller, *Chem. Rev.* **1998**, *98*, 675; b) S. Hong, T. J. Marks, *Acc. Chem. Res.* **2004**, *37*, 673; c) T. E. Müller, K. C. Hultsch, M. Yus, F. Foubelo, M. Tada, *Chem. Rev.* **2008**, *108*, 3795; d) K. D. Hesp, M. Stradiotto, *ChemCatChem* **2010**, *2*, 1192.
- [3] a) M. R. Gagné, T. J. Marks, *J. Am. Chem. Soc.* **1989**, *111*, 4108; b) M. R. Gagné, S. P. Nolan, T. J. Marks, *Organometallics* **1990**, *9*, 1716; c) M. R. Gagné, L. Brard, V. P. Conticello, M. A. Giardello, C. L. Stern, T. J. Marks, *Organometallics* **1992**, *11*, 2003; d) M. R. Gagné, C. L. Stern, T. J. Marks, *J. Am. Chem. Soc.* **1992**, *114*, 275.
- [4] For key contributions, see: a) P. J. Walsh, A. M. Baranger, R. G. Bergman, *J. Am. Chem. Soc.* **1992**, *114*, 1708; b) P. L. McGrane, M. Jensen, T. Livinghouse, *J. Am. Chem. Soc.* **1992**, *114*, 5459; c) M. A. Giardello, V. P. Conticello, L. Brard, M. Sabat, A. L. Rheingold,

- C. L. Stern, T. J. Marks, *J. Am. Chem. Soc.* **1994**, *116*, 10212; d) M. A. Giardello, V. P. Conticello, L. Brard, M. R. Gagne, T. J. Marks, *J. Am. Chem. Soc.* **1994**, *116*, 10241; e) Y. Li, T. J. Marks, *J. Am. Chem. Soc.* **1996**, *118*, 707; f) Y. Li, T. J. Marks, *J. Am. Chem. Soc.* **1998**, *120*, 1757; g) V. M. Arredondo, F. E. McDonald, T. J. Marks, *J. Am. Chem. Soc.* **1998**, *120*, 4871; h) V. M. Arredondo, S. Tian, F. E. McDonald, T. J. Marks, *J. Am. Chem. Soc.* **1999**, *121*, 3633; i) E. Haak, I. Bytschkov, S. Doye, *Angew. Chem.* **1999**, *111*, 3584; *Angew. Chem. Int. Ed.* **1999**, *38*, 3389; j) C. Li, R. K. Thomson, B. Gillon, B. O. Patrick, L. L. Schafer, *Chem. Commun.* **2003**, 2462; k) L. Ackermann, R. G. Bergman, R. N. Loy, *J. Am. Chem. Soc.* **2003**, *125*, 11956; l) J. Collin, J.-C. Daran, E. Schulz, A. A. Trifonov, *Chem. Commun.* **2003**, 3048; m) P. D. Knight, I. Munslow, P. N. O'Shaughnessy, P. Scott, *Chem. Commun.* **2004**, 894; n) D. V. Gribkov, K. C. Hultsch, *Angew. Chem.* **2004**, *116*, 5659; *Angew. Chem. Int. Ed.* **2004**, *43*, 5542; o) J. Collin, J.-C. Daran, O. Jacquet, E. Schulz, A. A. Trifonov, *Chem. Eur. J.* **2005**, *11*, 3455; p) D. V. Gribkov, K. C. Hultsch, F. Hampel, *J. Am. Chem. Soc.* **2006**, *128*, 3748; q) M. C. Wood, D. C. Leitch, C. S. Yeung, J. A. Kozak, L. L. Schafer, *Angew. Chem.* **2007**, *119*, 358; *Angew. Chem. Int. Ed.* **2007**, *46*, 354; r) A. L. Gott, A. J. Clarke, G. J. Clarkson, P. Scott, *Chem. Commun.* **2008**, 1422; s) I. Aillaud, J. Collin, C. Duhayon, R. Guillot, D. Lyubov, E. Schulz, A. A. Trifonov, *Chem. Eur. J.* **2008**, *14*, 2189; t) J. Hannedouche, I. Aillaud, J. Collin, E. Schulz, A. A. Trifonov, *Chem. Commun.* **2008**, 3552; u) A. V. Pawlikowski, A. Ellern, A. D. Sadow, *Inorg. Chem.* **2009**, *48*, 8020; v) L. E. N. Allan, G. J. Clarkson, D. J. Fox, A. L. Gott, P. Scott, *J. Am. Chem. Soc.* **2010**, *132*, 15308; w) A. L. Reznichenko, H. N. Nguyen, K. C. Hultsch, *Angew. Chem.* **2010**, *122*, 9168; *Angew. Chem. Int. Ed.* **2010**, *49*, 8984; x) D. C. Leitch, R. H. Platel, L. L. Schafer, *J. Am. Chem. Soc.* **2011**, *133*, 15453; y) K. Manna, S. Xu, A. D. Sadow, *Angew. Chem.* **2011**, *123*, 1905; *Angew. Chem. Int. Ed.* **2011**, *50*, 1865.
- [5] For Zn-catalyzed hydroamination reactions, see: a) A. Zulys, M. Dochnahl, D. Hollmann, K. Löhnwitz, J.-S. Herrmann, P. W. Roesky, S. Blechert, *Angew. Chem.* **2005**, *117*, 7972; *Angew. Chem. Int. Ed.*

- 2005, 44, 7794; b) M. Dochnahl, J.-W. Pissarek, S. Blechert, K. Löhnwitz, P. W. Roesky, *Chem. Commun.* **2006**, 3405; c) M. Dochnahl, K. Löhnwitz, J.-W. Pissarek, M. Biyikal, S. R. Schulz, S. Schön, N. Meyer, P. W. Roesky, S. Blechert, *Chem. Eur. J.* **2007**, 13, 6654; d) A. Mukherjee, T. K. Sen, P. K. Ghorai, P. P. Samuel, C. Schulzke, S. K. Mandal, *Chem. Eur. J.* **2012**, 18, 10530.
- [6] J. Haggin, *Chem. Eng. News* **1993**, 71, 23.
- [7] M. H. Chisholm, J. Gallucci, K. Phomphrai, *Chem. Commun.* **2003**, 48.
- [8] M. R. Crimmin, I. J. Casely, M. S. Hill, *J. Am. Chem. Soc.* **2005**, 127, 2042.
- [9] a) A. G. M. Barrett, M. R. Crimmin, M. S. Hill, P. B. Hitchcock, G. Kociok-Köhn, P. A. Procopiou, *Inorg. Chem.* **2008**, 47, 7366; b) A. G. M. Barrett, I. J. Casely, M. R. Crimmin, M. S. Hill, J. R. Lachs, M. F. Mahon, P. A. Procopiou, *Inorg. Chem.* **2009**, 48, 4445; c) M. R. Crimmin, M. Arrowsmith, A. G. M. Barrett, I. J. Casely, M. S. Hill, P. A. Procopiou, *J. Am. Chem. Soc.* **2009**, 131, 9670; d) M. Arrowsmith, M. S. Hill, G. Kociok-Köhn, *Organometallics* **2009**, 28, 1730; e) A. G. M. Barrett, C. Brinkmann, M. R. Crimmin, M. S. Hill, P. Hunt, P. A. Procopiou, *J. Am. Chem. Soc.* **2009**, 131, 12906; f) M. Arrowsmith, M. S. Hill, G. Kociok-Köhn, *Organometallics* **2011**, 30, 1291; g) M. Arrowsmith, M. R. Crimmin, A. G. M. Barrett, M. S. Hill, G. Kociok-Köhn, P. A. Procopiou, *Organometallics* **2011**, 30, 1493; h) C. Brinkmann, A. G. M. Barrett, M. S. Hill, P. A. Procopiou, *J. Am. Chem. Soc.* **2012**, 134, 2193.
- [10] For catalyzed reactions other than hydroamination, see: a) M. R. Crimmin, A. G. M. Barrett, M. S. Hill, P. A. Procopiou, *Org. Lett.* **2007**, 9, 331; b) M. R. Crimmin, A. G. M. Barrett, M. S. Hill, P. B. Hitchcock, P. A. Procopiou, *Organometallics* **2007**, 26, 2953; c) A. G. M. Barrett, T. C. Boorman, M. R. Crimmin, M. S. Hill, G. Kociok-Köhn, P. A. Procopiou, *Chem. Commun.* **2008**, 5206; d) J. R. Lachs, A. G. M. Barrett, M. R. Crimmin, G. Kociok-Köhn, M. S. Hill, M. F. Mahon, P. A. Procopiou, *Eur. J. Inorg. Chem.* **2008**, 4173; e) M. R. Crimmin, A. G. M. Barrett, M. S. Hill, P. B. Hitchcock, P. A. Procopiou, *Organometallics* **2008**, 27, 497.
- [11] R. D. Shannon, *Acta Crystallogr. Sect. A* **1976**, 32, 751.
- [12] Recently, several studies with highly efficient Mg catalysts for hydroamination reactions have been disclosed; see: a) X. Zhang, T. J. Emge, K. C. Hultsch, *Organometallics* **2010**, 29, 5871; b) J. F. Dunne, D. B. Fulton, A. Ellern, A. D. Sadow, *J. Am. Chem. Soc.* **2010**, 132, 17680; c) S. Tobisch, *Chem. Eur. J.* **2011**, 17, 14974; d) X. Zhang, T. J. Emge, K. C. Hultsch, *Angew. Chem.* **2012**, 124, 406; *Angew. Chem. Int. Ed.* **2012**, 51, 394.
- [13] a) S. Datta, P. W. Roesky, S. Blechert, *Organometallics* **2007**, 26, 4392; b) S. Datta, M. T. Gamer, P. W. Roesky, *Organometallics* **2008**, 27, 1207.
- [14] J. Jenter, R. Köppe, P. W. Roesky, *Organometallics* **2011**, 30, 1404.
- [15] J. S. Wixey, B. D. Ward, *Chem. Commun.* **2011**, 47, 5449.
- [16] J. S. Wixey, B. D. Ward, *Dalton Trans.* **2011**, 40, 7693.
- [17] Low (<10%) ee values were achieved in the cyclohydroamination of aminoalkenes with an enantiopure [(*S*)-Ph-bis(oxazoline)]CaN-(SiMe₃)₂(thf)₂ complex, but the complex probably decomposed under catalytic conditions; see: F. Buch, S. Harder, *Z. Naturforsch. B* **2008**, 63, 169.
- [18] a) M. S. Hill, P. B. Hitchcock, *Chem. Commun.* **2003**, 1758; b) A. G. Avent, M. R. Crimmin, M. S. Hill, P. B. Hitchcock, *Dalton Trans.* **2005**, 278; c) for a review, see: W. D. Buchanan, D. G. Allis, K. Ruhlandt-Senge, *Chem. Commun.* **2010**, 46, 4449.
- [19] a) F. Buch, J. Brettar, S. Harder, *Angew. Chem.* **2006**, 118, 2807; *Angew. Chem. Int. Ed.* **2006**, 45, 2741; b) J. Spielmann, S. Harder, *Chem. Eur. J.* **2007**, 13, 8928; c) J. Spielmann, S. Harder, *Eur. J. Inorg. Chem.* **2008**, 1480.
- [20] J. Spielmann, F. Buch, S. Harder, *Angew. Chem.* **2008**, 120, 9576; *Angew. Chem. Int. Ed.* **2008**, 47, 9434.
- [21] a) A. Weeber, S. Harder, H. H. Brintzinger, *Organometallics* **2000**, 19, 1325; b) F. Feil, S. Harder, *Organometallics* **2000**, 19, 5010; c) S. Harder, F. Feil, A. Weeber, *Organometallics* **2001**, 20, 1044; d) S. Harder, F. Feil, K. Knoll, *Angew. Chem.* **2001**, 113, 4391; *Angew. Chem. Int. Ed.* **2001**, 40, 4261; e) F. Feil, S. Harder, *Organometallics* **2001**, 20, 4616; f) S. Harder, F. Feil, *Organometallics* **2002**, 21, 2268; g) F. Feil, C. Müller, S. Harder, *J. Organomet. Chem.* **2003**, 683, 56; h) F. Feil, S. Harder, *Eur. J. Inorg. Chem.* **2003**, 3401; i) S. Harder, *Angew. Chem.* **2004**, 116, 2768; *Angew. Chem. Int. Ed.* **2004**, 43, 2714; j) D. F.-J. Piesik, K. Häbe, S. Harder, *Eur. J. Inorg. Chem.* **2007**, 5652.
- [22] a) Z. Zhong, P. J. Dijkstra, C. Birg, M. Westerhausen, J. Feijen, *Macromolecules* **2001**, 34, 3863; b) M. Westerhausen, S. Schneiderbauer, A. N. Kneifel, Y. Sörtl, P. Mayer, H. Nöth, Z. Zhong, P. J. Dijkstra, J. Feijen, *Eur. J. Inorg. Chem.* **2003**, 3432; c) M. H. Chisholm, J. C. Gallucci, K. Phomphrai, *Inorg. Chem.* **2004**, 43, 6717; d) D. J. Darensbourg, W. Choi, P. Ganguly, C. P. Richers, *Macromolecules* **2006**, 39, 4374; e) Y. Sarazin, R. H. Howard, D. L. Hughes, S. M. Humphrey, M. Bochmann, *Dalton Trans.* **2006**, 340; f) D. J. Darensbourg, W. Choi, C. P. Richers, *Macromolecules* **2007**, 40, 3521; g) M. G. Davidson, C. T. O'Hara, M. D. Jones, C. G. Keir, M. F. Mahon, G. Kociok-Köhn, *Inorg. Chem.* **2007**, 46, 7686; h) D. J. Darensbourg, W. Choi, O. Karroonnirun, N. Bhuvanesh, *Macromolecules* **2008**, 41, 3493; i) V. Poirier, T. Roisnel, J.-F. Carpentier, Y. Sarazin, *Dalton Trans.* **2009**, 9820; j) Y. Sarazin, V. Poirier, T. Roisnel, J.-F. Carpentier, *Eur. J. Inorg. Chem.* **2010**, 3423; k) Y. Sarazin, D. Roşca, V. Poirier, T. Roisnel, A. Silvestru, L. Maron, J.-F. Carpentier, *Organometallics* **2010**, 29, 6569; l) Y. Sarazin, B. Liu, T. Roisnel, L. Maron, J.-F. Carpentier, *J. Am. Chem. Soc.* **2011**, 133, 9069; m) B. Liu, T. Roisnel, Y. Sarazin, *Inorg. Chim. Acta* **2012**, 380, 2; n) B. Liu, T. Roisnel, J.-P. Guégan, J.-F. Carpentier, Y. Sarazin, *Chem. Eur. J.* **2012**, 18, 6289; o) B. Liu, V. Dorcet, L. Maron, J.-F. Carpentier, Y. Sarazin, *Eur. J. Inorg. Chem.* **2012**, 3023.
- [23] B. Liu, J.-F. Carpentier, Y. Sarazin, *Chem. Eur. J.* **2012**, 18, 13259.
- [24] B. Liu, T. Roisnel, J.-F. Carpentier, Y. Sarazin, *Angew. Chem.* **2012**, 124, 5027; *Angew. Chem. Int. Ed.* **2012**, 51, 4943.
- [25] Note that in lanthanide chemistry, the activity of a catalyst in an alkene hydroamination reaction generally increases with the size of the metal center.
- [26] See the Supporting Information for details.
- [27] Yet, solution ¹H NMR (¹J_{SiH}=162 Hz in a 4:1 mixture of [D₆]benzene and 1,2-C₆H₄F₂) and solid-state FTIR ($\bar{\nu}_{\text{SiH}}$ =2005, 1971, 1917 cm⁻¹) spectroscopic data were both compatible with the presence of stabilizing Sr...H-Si interactions.
- [28] The present study focuses solely on the intrinsic reactivity of the alkaline-earth complexes, and for this reason only, two of the most standard substrates were examined; therefore, the full extent of substrate scope was not explored and will be reported elsewhere.
- [29] Note that although commonly presented, the mechanism depicted in Scheme 2 is somewhat excessively simplistic, and the groups of Hill and Sadow have proposed alternative or more sophisticated mechanisms; for example, see references [9g] and [12b]. Note also that recent computational studies by Tobisch^[12c] have suggested that the Mg-catalyzed hydroamination proceeds through reversible olefin insertion and rate-determining protonolysis.
- [30] Reaction conditions: [Ae]₀/[B]₀=1:12, 20 μmol Ae, 80 °C, [D₆]benzene (0.4 mL).
- [31] J. Eppinger, M. Spiegler, W. Hieringer, W. A. Herrmann, R. Anwander, *J. Am. Chem. Soc.* **2000**, 122, 3080.
- [32] A. G. M. Barrett, M. R. Crimmin, M. S. Hill, G. Kociok-Köhn, J. R. Lachs, P. A. Procopiou, *Dalton Trans.* **2008**, 1292.
- [33] P. N. O'Shaughnessy, P. Scott, *Tetrahedron: Asymmetry* **2003**, 14, 1979.
- [34] K. C. Hultsch, F. Hampel, T. Wagner, *Organometallics* **2004**, 23, 2601.
- [35] No information is available for the solid-state structure of **8**, but DOSY NMR spectroscopic data were consistent with a monomeric complex in solution.
- [36] For the solid-state structures and solution behavior of these Ca complexes, see reference [22n].
- [37] On account of their inactivity under our standard conditions, ¹H NMR spectroscopic kinetic monitoring was not performed for [(LO³)CaN(SiMe₂H)₂] (**9**) nor for the Sr and Ba analogues.

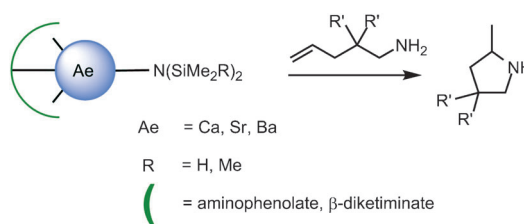
- [38] a) R. D. Cannon, J. S. Stillman, *Inorg. Chem.* **1975**, *14*, 2202; b) R. D. Cannon, J. S. Stillman, *Inorg. Chem.* **1975**, *14*, 2207.
- [39] A. G. Avent, M. R. Crimmin, M. S. Hill, P. B. Hitchcock, *Dalton Trans.* **2004**, 3166.
- [40] K. Takaki, T. Kamata, Y. Miura, T. Shishido, K. Takehira, *J. Org. Chem.* **1999**, *64*, 3891.
- [41] J. F. Dunne, S. R. Neal, J. Engelkemier, A. Ellern, A. D. Sadow, *J. Am. Chem. Soc.* **2011**, *133*, 16782.
- [42] The solid-state structure of **16** was determined by X-ray diffraction crystallography, and it very closely resembled [(BDI)SrN(SiMe₃)₂{H₂N(CH₂)₂OMe}],^[9g] with a five-coordinated Sr center bearing a chelating H₂N(CH₂)₂OMe bidentate ligand instead of the two THF molecules found in **12**. The Si-N-Si angle 136.0° in **16** was noticeably wider than in [(BDI)SrN(SiMe₃)₂{H₂N(CH₂)₂OMe}] (123.5°) or in **12** (127.4°); whereas [(BDI)SrN(SiMe₃)₂{H₂N(CH₂)₂OMe}] was in 75:25 equilibrium with [(BDI)Sr{HN(CH₂)₂OMe}] through amine/amide exchange,^[9g] there was no spectroscopic evidence for such an equilibrium involving **16** and [(BDI)Sr{HN(CH₂)₂OMe}]. We attributed the specific behavior of **16** to the low basicity of the N-(SiMe₂H)₂⁻ ion with respect to those of the N(SiMe₃)₂⁻ and MeO-(CH₂)₂NH⁻ ions. Similarly, different behavior in solution was observed for the Ca complexes **11** and [(BDI)CaN(SiMe₃)₂(thf)]. Whereas the formation of the dimeric [(BDI)Ca{μ-NH-(CH₂)₂OMe}]₂ occurred readily at room temperature upon treatment of [(BDI)CaN(SiMe₃)₂(thf)] with 2-methoxyethylamine,^[37] only the amine adduct **15** was obtained by using **11** as the starting material. Besides, heating **15** to 80°C quantitatively afforded the product of dehydrogenative N-Si coupling, that is, [(BDI)CaN-(SiMe₂H)(SiMe₂HN(CH₂)₂OMe)].
- [43] A. W. Addison, T. N. Rao, J. Reedijk, J. van Rijn, G. C. Verschoor, *J. Chem. Soc. Dalton Trans.* **1984**, 1349.
- [44] Reaction conditions: 20 μmol of Ca complex, [D₆]benzene (0.4 mL), T=80°C.
- [45] Y. Tamaru, M. Hojo, H. Higashimura, Z. Yoshida, *J. Am. Chem. Soc.* **1988**, *110*, 3994.
- [46] J. M. Boncella, C. J. Coston, J. K. Cammack, *Polyhedron* **1991**, *10*, 769.
- [47] a) V. Poirier, T. Roisnel, J.-F. Carpentier, Y. Sarazin, *Dalton Trans.* **2011**, *40*, 523; b) S. Groysman, E. Sergeeva, I. Goldberg, M. Kol, *Inorg. Chem.* **2005**, *44*, 8188; c) S. Itoh, H. Kumei, S. Nagatomo, T. Kitagawa, S. Fukuzumi, *J. Am. Chem. Soc.* **2001**, *123*, 2165.
- [48] J. E. Parks, R. H. Holm, *Inorg. Chem.* **1968**, *7*, 1408.
- [49] a) G. M. Sheldrick, SHELXS-97, Program for the Determination of Crystal Structures, University of Göttingen (Germany), **1997**; b) G. M. Sheldrick, SHELXL-97, Program for the Refinement of Crystal Structures, University of Göttingen (Germany), **1997**.

Received: October 5, 2012
Published online: ■ ■ ■, 0000

Homogeneous Catalysis

B. Liu, T. Roisnel, J.-F. Carpentier,*
Y. Sarazin* ■■■-■■■

Cyclohydroamination of Aminoalkenes Catalyzed by Disilazide Alkaline-Earth Metal Complexes: Reactivity Patterns and Deactivation Pathways



Playing a role: Phenolate and β -diketiminate disilazide complexes of the large alkaline-earth metals (Ca, Sr, and Ba) have been employed as competent catalysts for the cyclohydroamination of terminal aminoalkenes (see scheme). Trends regarding the catalytic

activity of these complexes have been established and allow the discrimination between metal, ligand framework, and amido groups. A specific deactivation pathway has been identified, and several model compounds have been used for stoichiometric investigations.